Atmos. Chem. Phys. Discuss., 13, 4221–4287, 2013
www.atmos-chem-phys-discuss.net/13/4221/2013/
doi:10.5194/acpd-13-4221-2013

Atmospheric Chemistry and Physics
Discussions
Open Access

Stratospheric lifetimes of CFC-12, CCl_4, CH_4, CH_3Cl and N_2O from measurements made by the Atmospheric Chemistry Experiment-Fourier Transform Spectrometer (ACE-FTS)

A. T. Brown[1], C. M. Volk[2], M. R. Schoeberl[3], C. D. Boone[4], and P. F. Bernath[5,6]

[1]Department of Physics, University of York, Heslington, YO10 5DD, UK
[2]Department of Physics, University of Wuppertal, 42119 Wuppertal, Germany
[3]Science and Technology Corporation, Lanham, MD 20706, USA
[4]Department of Chemistry, University of Waterloo, Ontario, Canada
[5]Department of Chemistry and Biochemistry, Old Dominion University, VA, USA
[6]Department of Chemistry, University of York, Heslington, YO10 5DD, UK

Received: 24 January 2013 – Accepted: 30 January 2013 – Published: 14 February 2013

Correspondence to: A. T. Brown (alex.brown@york.ac.uk)

Published by Copernicus Publications on behalf of the European Geosciences Union.

Abstract

Long lived halogen-containing compounds are important atmospheric constituents since they can act both as a source of chlorine radicals, which go on to catalyse ozone loss, and as powerful greenhouse gases. The long term impact of these species on the ozone layer is dependent on their stratospheric lifetimes. Using observations from the Atmospheric Chemistry Experiment Fourier Transform Spectrometer (ACE-FTS) we present calculations of the stratospheric lifetimes of CFC-12, CCl_4, CH_4, CH_3Cl and N_2O. The lifetimes were calculated using the slope of the tracer-tracer correlation of these species with CFC-11 at the tropopause. The correlation slopes were corrected for the changing atmospheric concentrations of each species based on age of air and CFC-11 measurements from samples taken aboard the Geophysica aircraft – along with the effective linear trend of the VMR from tropical ground-based AGAGE sites. Stratospheric lifetimes were calculated using a CFC-11 lifetime of 45 yr. These calculations produced values of 113 + (–)26(18) yr (CFC-12), 35 + (–)11(7) yr (CCl_4), 195 + (–)75(42) yr (CH_4), 69 + (–)65(23) yr (CH_3Cl) and 123 + (–)53(28) yr (N_2O). The errors on these values are the weighted 1-σ non-systematic errors. The stratospheric lifetime of CH_3Cl represents the first calculations of the stratospheric lifetime of CH_3Cl using data from a space based instrument.

1 Introduction

Catalytic stratospheric ozone destruction occurs through the formation of halogen, nitrogen and hydrogen radicals. The halogen and nitrogen source gases also play a role in global radiative transfer by blocking outgoing infrared radiation. In the case of halogen source gases, the long tropospheric lifetimes of many halogen-containing species allow them to reach the stratosphere through the upwelling tropical circulation. Once in the stratosphere they undergo photolysis and the halogen atoms which they contain are released into the surrounding atmosphere. Chlorine and bromine atoms released

ACPD
13, 4221–4287, 2013

into the stratosphere catalyse ozone destruction. Fluorine atoms react rapidly to form stable HF. Chlorine-containing molecules typically absorb infrared radiation in the 650–780 cm^{-1} region (Lide, 1990; http://nwir.pnl.gov/), which is partly masked by CO_2 and water vapour absorption. Despite this, species such as CCl_4 have large global warming potentials, for example CCl_4 has a global warming potential 1400 times larger than CO_2 (Solomon, 2007). C–F bonds typically absorb radiation in the 1000–1300 cm^{-1} region (http://nwir.pnl.gov/; Lide, 1990), a region which is relatively clear from atmospheric absorption from other species making fluorine-containing molecules powerful greenhouse gases. The emissions of many halogen-containing species are now limited under the Montreal Protocol (UNEP, 2009). The Montreal Protocol has been successful in both reducing the emissions of these species (Brown et al., 2011) and slowing the rate of ozone loss (Mäder et al., 2010). The reduction in the emission of ozone depleting substances has also had an effect in reducing the concentration of greenhouse gases (Velders et al., 2007).

A full analysis of ozone destruction must also take species such as N_2O, which is the major source of stratospheric NO and NO_2, and CH_4, which acts as a sink for atmospheric OH, into account. The long term impact of these species on the environment is determined by their atmospheric lifetimes. Accurate estimates of atmospheric lifetimes of species which are directly and indirectly involved in stratospheric ozone loss are therefore vital. In particular, atmospheric lifetimes are used to set environmental policies on the emissions of ozone depleting substances and greenhouse gases. N_2O and methane are also greenhouse gases; furthermore methane contributes to stratospheric water vapour that can affect surface temperatures (Solomon, 2007).

The 2010 scientific assessment of ozone depletion report from the World Meteorology Organisation (WMO) (Montzka et al., 2011) highlighted problems with the current lifetimes of some halogen-containing species such as carbon tetrachloride (CCl_4). Atmospheric concentrations of CCl_4 are declining more slowly than expected which could be caused by an unreliable atmospheric lifetime (Montzka et al., 2011). This has led to the formation of the Stratospheric-Troposphere Processes And their Role

ACPD
13, 4221–4287, 2013

in Climate (SPARC) lifetimes reassessment project. The aim of the re-evaluation is to estimate the numerical values of the lifetimes and the associated errors, assess the influence of different lifetime definitions and assess the effect of changing climate on lifetimes. The SPARC science report will be published by spring 2013 and will form the basis for the 2014 WMO Ozone Assessment (http://www.sparc-climate.org/activities/lifetime-halogen-gases/).

There are a number of methods for calculating the stratospheric lifetimes of long lived gases using satellite measurements. Stratospheric lifetimes can be calculated using a combination of satellite measurements and an atmospheric model. Satellite measurements are used to calculate the global atmospheric burden of a species. Subsequently, model data can be used to calculate the loss rates for the species from photolysis and chemical reaction. The instantaneous lifetime of a species is simply the global atmospheric burden divided by the sum of the loss rates (Johnston et al., 1979; Minschwaner et al., 1998). In-situ measurements using balloon and aircraft borne instruments can be used to calculate stratospheric lifetimes of a number of long lived species using correlations with CFC-11 (Volk et al., 1997; Bujok et al., 2001; Laube et al., 2012). This method relies on accurate knowledge of the lifetime of CFC-11. Recent calculations of the lifetime of CFC-11, carried out using model data, have produced values between 56 and 64 yr (Douglass et al., 2008), whilst older estimates suggest a lifetime of 45 yr (Prinn et al., 1999). This uncertainty in the lifetime of CFC-11 therefore has a significant effect on the stratospheric lifetime estimates of a number of other halogen-containing species. If satellite data is to be used to carry out this analysis it should have sufficiently high vertical resolution to be able to extrapolate the slope of the correlation to the tropopause. Limb sounding satellite borne instruments, such as the Atmospheric Chemistry Experiment (ACE) and the Michelson Interferometer for Passive Atmospheric Sounding (MIPAS), have sufficiently high vertical resolution to be used for this method of lifetime calculation.

This paper presents new stratospheric lifetime estimates for CFC-12, CCl_4, CH_4, CH_3Cl and N_2O calculated from correlations with CFC-11 using data from Atmospheric

ACPD
13, 4221–4287, 2013

Chemistry Experiment Fourier Transform Spectrometer (ACE-FTS). For CFC-12, CCl_4 and N_2O, which have no chemical sink in the troposphere, these lifetimes correspond to the global lifetime with respect to atmospheric removal.

2 Atmospheric chemistry experiment

Launched by NASA on board the Canadian satellite SCISAT-1 in August 2003, the Atmospheric Chemistry Experiment Fourier Transform Spectrometer (ACE-FTS) was designed to study "the chemical and dynamical processes that control the distribution of ozone in the stratosphere and upper troposphere" (Bernath, 2006). ACE-FTS was designed to build on the success of the Atmospheric Trace Molecule Spectroscopy (ATMOS) instrument. ATMOS flew on four separate shuttle flights, between 1985 and 1993, and pioneered space based observations of a number of halogenated gases (Irion et al., 2002).

The ACE-FTS is a high resolution (0.02 cm^{-1}) spectrometer operating between 750 and 4400 cm^{-1}. ACE-FTS is a solar occultation instrument; a series of atmospheric absorption spectra are measured at a number of tangent heights during sunrise and sunset. Currently this method of measurement allows the retrieval of vertical profiles with high vertical resolution (2–3 km near the tropopause) of over 30 molecules (http://www.ace.uwaterloo.ca). The methodology used to retrieve the VMRs of the different molecules from the ACE-FTS spectra is outlined by Boone et al. (Boone et al., 2005). ACE-FTS has almost global coverage from the Antarctic to the Arctic due to the circular low earth orbit with an inclination of 74° of SCISAT-1 (Bernath et al., 2005). The instrument has been in operation for eight years, offering long term observations of the volume mixing ratios of a number of atmospheric gases.

ACPD
13, 4221–4287, 2013

3 Method

The lifetime calculations presented in this paper were calculated following the method laid out by Volk et al. (1997) based on the theoretical work of Plumb and Ko (1992) and Plumb (1996). In this section a brief outline of the method will be given; for a more complete discussion the reader is directed to the aforementioned paper.

The stratospheric lifetimes (τ_a, τ_b) of two long lived species, a and b, are related by the ratio of their average atmospheric Volume Mixing Ratio (VMR), $\overline{\sigma}$, and the slope of the correlation at the extratropical tropopause ($d\chi_a/d\chi_b$). In this paper we follow the convention of Volk et al. (1997), where χ refers to the (transient) mixing ratios and σ represents the mixing ratios corresponding to a steady state situation with the same tropopause mixing ratio.

$$\frac{\tau_a}{\tau_b} = \frac{\dfrac{\overline{\sigma_a}}{\overline{\sigma_b}}}{\left.\dfrac{d\sigma_a}{d\sigma_b}\right|_{\text{tropopause}}} \tag{1}$$

This method can be used to calculate the relative lifetime of a long-lived species, a, assuming that the lifetime of a second long-lived species, b, is known. Conventionally lifetimes derived in this manner are calculated relative to CFC-11. Calculations are complicated by the fact that the observed VMRs (χ) of the species used in this study are changing independently of one another, while Eq. (1) requires steady-state quantities (σ). For the species considered here, the average VMRs for steady-state ($\overline{\sigma_l}$) may well be approximated with the observed ones ($\overline{\chi_l}$) as the VMRs are nearly constant in the well-mixed troposphere that accommodates most of the species' burden. The transient correlation slopes at the tropopause, however, generally differ significantly from those in steady state.

ACPD
13, 4221–4287, 2013

$$\left.\frac{\mathrm{d}\sigma}{\mathrm{d}\Gamma}\right|_{\Gamma=0} = \frac{\left(\left.\frac{\mathrm{d}\chi}{\mathrm{d}\Gamma}\right|_{\Gamma=0} + \gamma_0\sigma_0\right)}{(1-2\gamma_0\Lambda)} \quad (2)$$

$$\chi_0(t') = \chi_0(t)\left[1 + b(t'-t) + c(t'-t)^2\right] \quad (3)$$

$$\gamma_0 = b - 2\Lambda c \quad (4)$$

Volk et al. (1997) used a correction factor which was calculated using the correlation between the VMR of a species and the age-of-air above the tropopause ($\mathrm{d}\chi/\mathrm{d}\Gamma$). The correction of $\mathrm{d}\chi/\mathrm{d}\Gamma$ to account for growth in the VMR of a species ($\mathrm{d}\sigma/\mathrm{d}\Gamma$ – Eq. 2) is complicated by a number of factors. The atmospheric growth rates of individual species are not necessarily linear. This necessitates the calculation of the effective linear growth rate (γ_0), and knowledge of the VMR of a species at the tropopause (σ_0). In order that γ_0 may be calculated, a long term tropospheric data set for each species is required. A polynomial curve can be fitted to this data from the beginning of the time series to a specific reference time when the measurements were made (for example if the ACE-FTS measurement was made in 2009, t = 2009, t' = year in which the individual ground based measurement in the time series was made). The fit coefficients, b and c, (Eq. 3) can be used to calculate the γ_0 from Eq. (4). The second factor which complicates the process comes from the stratospheric age of air spectrum. The Λ factor in Eqs. (2) and (4) is the ratio of the squared width of the age spectrum to the mean age and accounts for the effects of the finite width of the age of air spectrum (Volk et al., 1997). For this work we have chosen to use a value of 1.25 yr for Λ following the work of Volk et al. (1997) and Laube et al. (2012). Rather than evaluating Eq. (2) for each species as done in Volk et al. (1997) we here combine it for two tracers a and b and substitute $\mathrm{d}\chi_a/\mathrm{d}\Gamma$ with $\mathrm{d}\chi_a/\mathrm{d}\chi_b \cdot \mathrm{d}\chi_b/\mathrm{d}\Gamma$, so that only the gradient with respect to mean age of tracer species b is required. This results in the following relation between the steady-state tracer-tracer correlation slope ($\mathrm{d}\sigma_a/\mathrm{d}\sigma_b$) required in Eq. (1) and the observed transient slope ($\mathrm{d}\chi_a/\mathrm{d}\chi_b$):

ACPD
13, 4221–4287, 2013

$$\left.\frac{d\sigma_a}{d\sigma_b}\right|_{\text{tropopause}} = \frac{\left.\frac{d\chi_a}{d\chi_b}\right|_{\text{tropopause}} \cdot \left.\frac{d\chi_b}{d\Gamma}\right|_{\Gamma=0} + \gamma_{0a}\sigma_{0a}}{\left.\frac{d\chi_b}{d\Gamma}\right|_{\Gamma=0} + \gamma_{0b}\sigma_{0b}} \cdot \frac{1-2\gamma_{0b}\Lambda}{1-2\gamma_{0a}\Lambda} \tag{5}$$

The slope of the correlation of mean age against CFC-11 at the tropopause required in Eq. (5) was calculated by Laube et al. (2012) based on laboratory analysis of CFC-11 and SF_6 in whole air samples taken on board the Geophysica aircraft in October 2009 and January 2010. These calculations produced a value of $-20.6 \pm 4.3\,\text{ppt}\,\text{yr}^{-1}$ for early 2010 for the slope at the tropopause. This value has been scaled by the effective linear growth rate (γ_0) of CFC-11 during this time (the values for which can be seen in Table 2). The values for the age of air slopes can be seen in Table 1. The use of the Laube et al. (2012) CFC-11 versus age of air slopes facilitates the comparisons of lifetimes calculated from ACE with those derived from the Geophysica samples by Laube et al. (2012). Initially we tested whether a correlation between model age data and ACE CFC-11 could contain the slopes but it was found that this was not the case.

4 Results and discussion

ACE-FTS data were divided into 24 separate data bins dependent on their stratospheric season and year. The data was first divided into 4 bins which corresponded with Northern Hemisphere stratospheric Winter (NHW), Northern Hemisphere stratospheric Summer (NHS), Southern Hemisphere stratospheric Winter (SHW) and Southern Hemisphere stratospheric Summer (SHS). These four bins were defined by the month in which the occultations were made in the following manner:

ACPD
13, 4221–4287, 2013

Northern Hemisphere Stratospheric Winter	November – December – January – February – March – April
Northern Hemisphere Stratospheric Summer	May* - June – July – August – September – October*
Southern Hemisphere Stratospheric Winter	May – June – July – August – September – October
Southern Hemisphere Stratospheric Summer	November* – December – January – February – March – April*

The months marked with asterisks are not truly stratospheric summer months; they were selected to increase the sample size used in this study. The NHW bin for 2005 would include data from November and December 2004 and from January, February, March and April 2005. Likewise, SHS 2005 included November and December 2004 and January, February, March and April 2005.

In the tropics, there is large scale upwelling through the tropopause to higher altitudes and further up in relative isolation from mid-latitudes, resulting in tropical correlation curves different from those in the extra-tropical surf zone (e.g. Volk et al., 1996). Tropical correlations thus reflect local rather global sources and sinks and are thus unrelated to stratospheric lifetimes (Plumb, 1996). In the higher latitudes, the polar vortex causes stratospheric air to subside in isolation from mid-latitudes and correlation curves within the vortex develop separately from those at mid-latitudes over the course of the winter (e.g. Plumb, 2007), thus making occultations within the polar vortex unsuitable for the derivation of stratospheric lifetimes. Tropical and polar latitudes thus act as lower and upper limits for the latitudes from which data can be used in this study. The latitudes used in this study run from above the tropics, 30° N/S, to 70° N/S. Measurements made within the polar vortex appeared as outliers to the overall data

ACPD
13, 4221–4287, 2013

and were removed as they fell outside of the median absolute deviation (MAD) filter. In this way both the tropical and the polar-regions are avoided. The division of the data into Northern and Southern Hemisphere was designed to test whether there is any hemispheric dependence in the calculated lifetimes. By dividing the data seasonally the sensitivity of the calculated lifetimes to seasonal variation was also to be explored. Since the background VMR of these species varies annually the data was divided into additional bins inside of the four mentioned previously. These bins were separated by the year in which the occultations were made.

Once the data had been divided into the relevant bin, the data within the bins was filtered. Outlying data were removed from the ACE-FTS VMR profiles by excluding data whose deviation from the median was greater than 2.5 times the median absolute deviation (MAD) at each altitude. A MAD filter is an effective way to remove outlying data since the MAD is less susceptible to outliers than the standard deviation. As has been mentioned previously, data within the polar vortex was outside these parameters and was therefore discarded during this stage of filtering. A final round of filtering removed data below the tropopause using tropopause altitudes from the ACE derived meteorological product (DMPs). Each ACE occultation has a unique DMP which presents the altitude of the tropopause at the latitude, longitude and local time of the occultation.

4.1 CFC-11 correlations

Mean correlation curves were produced for the correlations of each species vs CFC-11. The mean correlation curves were calculated using the mean of the data in non-overlapping windows which were 2 ppt of CFC-11 wide. The error on the mean of this data in both x and y (where y is CFC-11 and x is the correlating species) is the standard error on the mean. These windows ran the entire range of the CFC-11 data beginning at the minimum concentration and moving along every 2 ppt until the maximum concentration value had been passed. Once a mean correlation curve had been produced the slope of the data within a moving window of 80 ppt of CFC-11 was calculated using a linear least squared fit which took both the error in the CFC-11 and the correlating species mean into account. After measuring the slope of the data the window would be moved forwards by 5 ppt and the slope of the data would be calculated again. The procedure started 80 ppt of CFC-11 below the minimum CFC-11 VMR, providing a blank first reading. This procedure continued until the window was 80 ppt larger than the maximum CFC-11 VMR. Once this procedure had been carried out data from windows corresponding to a CFC-11 VMR of less than 120 ppt were discarded and a second degree polynomial was fit to the remaining data. The data was weighted using the square of the inverse fitting errors on each point from the previous step. The aim of these calculations was to extrapolate the slope of the correlation to the tropopause. Removing data below 120 ppt of CFC-11 ensured that the polynomial fit would not be biased towards the higher altitudes. On the other hand, the range of the fit (120 to ~ 220 ppt) ensured that the extrapolated slope at the tropopause would not be unduly affected from points directly at the tropopause where complex mixing from the troposphere can cause the observed correlation to break down. Examples of the correlation plots and slope calculations can be seen in Fig. 1, the remaining plots can be found in Appendix B (Figs. B1 to B21). The uncertainties quoted in this work are the statistical uncertainties of the calculated results. The systematic errors, which may be introduced during the retrieval process, are not included in these calculations. This will lead to a small underestimation in error on the final results quoted here.

Fluxes of chemical species into the stratosphere from the tropopause are not constant and are prone to change as long as the species are not in steady state. This produces a curving effect in the correlations around the tropopause that can be clearly seen in Fig. 1. The method employed in this paper requires the knowledge of the slope of the stratospheric tracer-tracer correlation at the tropopause. The slope of the correlation at the tropopause was calculated using the equation derived from the polynomial fit along with the mean CFC-11 VMR at the tropopause. Following the work of Volk et al. (1997) errors on the fit were calculated using a bootstrap method (Efron et al., 1991) and scaled using the number of independent points used in the extrapolation fit.

ACPD
13, 4221–4287, 2013

The slopes at the tropopause are shown in Table 1 in the section A of the appendix along with a plot of these slopes for comparison. There are 3 bins with no correlation data, NHW 2005, SHW 2005 and NHW 2009. In these bins problems with the retrieval program, used to retrieve VMR from ACE-FTS spectra, caused a failure in the retrieval of CFC-11. Work is on-going at this time to rectify this problem. Correlations between CFC-12 and CFC-11 produce slopes that range between 0.61 ± 0.04 and 1.25 ± 0.1. With a median (of all 24 bins) of 0.99 and a standard deviation of 0.19 these data exhibit good self-consistency. The slopes of the CH_3Cl correlation show a significant spread with a maximum of 3.16 ± 2.25 and a minimum of 0.68 ± 0.39. The slopes have a median of 1.60 and a standard deviation of 0.65. CCl_4 has a large spread of slopes with a median of 0.59 and a standard deviation of 0.23. The maxima and minima of this data are 1.24 ± 0.26 and 0.18 ± 0.11. Both CH_4 and N_2O show relatively wide spreads of values with medians of 2026 and 577 and standard deviations of 914 and 178, respectively. One source of variation of the CH_3Cl and CH_4 could be the flux of species across the tropopause, e.g. due to seasonal or inter-annual variations in tropospheric growth, leading to changes to the correlation slopes in the lowest part of the stratosphere.

The effective linear growth rate (γ_0 – Eq. 5) was calculated using monthly global means from the Advanced Global Atmospheric Gases Experiment (AGAGE) network (Prinn et al., 2000, 2001) for CFC-11 (Cunnold et al., 2002), CFC-12 (Cunnold et al., 1997), CCl_4 (Simmonds et al., 1998), CH_4 (Cunnold et al., 2002; Rigby et al., 2008), CH_3Cl (Simmonds et al., 2004; Cox et al., 2003) and N_2O (Prinn et al., 1990).

The VMRs at the tropopause (σ_0) were calculated by removing any data below 3 km below the tropopause and any data which lay above the tropopause. The remaining data was used to calculate a mean VMR which represented σ_0; these values can be seen in Table 2 of Appendix A. The corrected correlations, calculated using Eq. (7), can be found in Table 3 of Appendix A.

ACPD
13, 4221–4287, 2013

4.2 Lifetime calculations

The annual global mean atmospheric VMR ($\overline{\sigma}$) of each species was calculated using ACE-FTS profiles of the VMR (σ) and atmospheric pressure (P). In this case pressure is being used as a proxy for density. Whilst using pressure will weight the lower stratosphere less than it deserves, giving a higher bias in the atmospheric means, this effect will not be larger than the errors which are currently assigned to the means. Mean VMR profiles were calculated for each species in 15° latitude bins. Profiles were extended from their lowest point to the ground by assuming a constant VMR. Each VMR value was weighted by the corresponding pressure; this allowed a weighted mean to be calculated using Eq. (7). The global mean atmospheric VMRs were then calculated by weighting the pressure weighted means from the latitude bins using the cosine of the latitude. This was done since the majority of the mass of the global atmosphere is contained in the tropical troposphere. The results of this analysis can be seen in Table 4 of Appendix A.

$$\overline{\sigma} = \frac{\sum P_i \sigma_i}{\sum P_i} \tag{6}$$

Calculations were carried out using a CFC-11 lifetime of 45 yr for ease of comparisons with previous studies. Theses lifetimes are presented in Table 3 (a plot of these slopes for comparison can be found in Appendix A). The final error on the calculated lifetimes is a combination of the errors from each step of the calculation. The lifetimes calculated for CH_3Cl and CH_4 show significant variation between the calculated lifetimes. None of the other species display such significant variation and so it is unlikely that this variation is due to variation in the transport across the tropopause.

Weighted mean lifetimes were calculated for each seasonal and hemispheric combination. The means were weighted using the inverse square of the largest error on each calculated lifetime. Whilst the mean lifetimes calculated from the Northern Hemisphere (NH in Table 4) are longer than those calculated from the Southern Hemisphere (SH

ACPD
13, 4221–4287, 2013

in Table 4) this is not always the case (for example CCl_4 and CH_4) and so it is hard to draw any solid conclusions from this fact. Only CH_4 exhibits a variation between the hemispherically calculated lifetimes which is larger than the errors on the lifetimes. Generally lifetimes calculated using summer data are smaller than those calculated using winter data. Once more however this is not always the case; the calculated lifetimes using winter data of both N_2O and CH_4 are smaller than those calculated using summer data. Variation between the seasonally calculated lifetimes is in fact smaller than the error. Vertical mixing in the stratosphere occurs due to breaking Rossby waves found during the winter in the stratosphere (Plumb, 2002). The implication of this is that mixing occurs at a greater rate in the winter stratosphere than in the summer stratosphere. The mean lifetimes calculated here suggest that this phenomenon has not affected our stratospheric lifetime calculations. Since neither the season nor the hemisphere appears to have a significant effect on our results it is possible to calculate a total weighted mean. The results of these calculations can be seen in Table 4. The error on these results is the weighted standard deviation using the reciprocal of the square of the error. It should be noted that in the case of the result for the Northern Hemisphere summer CH_3Cl calculated lifetime, due to problems caused within the fitting program it was only possible to produce one calculated lifetime for this bin. The mean lifetime reported here is therefore this calculated lifetime and associated error. As has been noted previously the errors quoted here are the statistical uncertainties of the calculated results. The systematic errors are not accounted for in the quoted errors and so some of the seasonal and hemispheric variation is likely due to a small underestimation of these errors.

The calculated lifetimes of CFC-12, CCl_4 and N_2O – 113 + (–)26(18), 35 + (–)11(7) and 123 + (–)53(28) yr, respectively – are within error of the lifetimes quoted by the WMO/IPCC – 100 (Montzka et al., 2011), 35 (Montzka et al., 2011) and 114 (Solomon, 2007) years. The lifetime calculated for methane, of 195 + (–)75(42) yr, is significantly larger than that calculated by (Volk et al., 1997) of 103±11 yr. It is likely that the variation in the correlation slopes in the lower stratosphere is due to changes in the flux of CH_4

ACPD
13, 4221–4287, 2013

across the troposphere. This could lead to artificially high calculated lifetimes which would influence the final mean lifetime. The stratospheric lifetime of CH_3Cl of 69 + (−)65(23) yr, reported here, represents the first calculation of the stratospheric lifetime of CH_3Cl using data from a space based instrument.

Recent model simulations have suggested CFC-11 lifetimes of between 56 and 64 yr (Douglass et al., 2008), differing from the older value of 45 yr which was used in the 2010 WMO report (Montzka et al., 2011). Changes to the lifetime of CFC-11 would naturally have an effect on the calculated lifetime of atmospheric species calculated using correlations with CFC-11. For example using the range of CFC-11 lifetimes noted above produces a lifetime for CFC-12 which lies between 125 and 143 yr. The ratio of the lifetime of CFC-12, CCl_4, CH_4, CH_3Cl and N_2O to CFC-11 are shown in Table 5. These values can be multiplied by the lifetime of CFC-11 to calculate the stratospheric lifetime of the species of interest. If the lifetime of CFC-11 is constrained further these ratios can be used to calculate new relative lifetimes.

5 Conclusions

This paper presents calculations for the stratospheric lifetimes of CFC-12, CCl_4, CH_4, CH_3Cl and N_2O. The calculations were carried out using measurements made by the Atmospheric Chemistry Experiment Fourier Transform Spectrometer (ACE-FTS). The aim of this project was not only to calculate the stratospheric lifetimes of the species in question but also to test the assumptions which are intrinsic to these calculations. These assumptions are that there should be no hemispheric dependence in the calculated lifetimes and that there should be no seasonal dependence in the calculated lifetimes. To do this the data was divided into 24 bins representing stratospheric summer and winter in the Northern and Southern Hemisphere for years between 2005 and 2010.

Stratospheric lifetimes were calculated using the slope of the correlation with CFC-11 at the tropopause. The stratified nature of the stratosphere ensured that the

Discussion Paper | Discussion Paper | Discussion Paper | Discussion Paper |

ACPD

13, 4221–4287, 2013

Stratospheric lifetimes of CFC-12, CCl_4, CH_4, CH_3Cl and N_2O

A. T. Brown et al.

correlations had to be corrected for changing atmospheric concentrations of each species. Stratospheric lifetimes were calculated using a lifetime of 45 years for CFC-11. CFC-12 and N_2O are chemically inert in the troposphere and so their stratospheric lifetimes represent their atmospheric lifetimes. Calculated lifetimes showed no significant hemispheric or seasonal dependency. This suggested that for relative lifetime calculations the hemispheres are identical throughout the year. Individual lifetimes calculated for CH_3Cl and CH_4 displayed a large spread of values. The cause of this large spread is likely to be the reactions of these species with OH which is a more important sink for these species than photolysis.

Weighted means were calculated by weighting the individual lifetimes by the reciprocal of the square of their error. These calculations produced values of 113 + (–)26(18) yr (CFC-12), 35 + (–)11(7) yr (CCl_4), 195 + (–)75(42) yr (CH_4), 69 + (–)65(23) yr (CH_3Cl) and 123 + (–)53(28) yr (N_2O). The calculated lifetimes of CFC-12, CCl_4 and N_2O are within error of the lifetimes quoted by the WMO/IPCC – 100 (Montzka et al., 2011), 35 (Montzka et al., 2011) and 114 (Solomon, 2007) yr. The lifetime calculated for methane, of 195 + (–)75(42) yr, is significantly larger than that calculated by (Volk et al., 1997) of 103 ± 11 yr. These lifetimes are relative to the lifetime of CFC-11 (45 yr), thus if the lifetime of CFC-11 changes so will the lifetime of these species. The ratios between the lifetime of CFC-12, CCl_4, CH_4, CH_3Cl and N_2O and CFC-11 were also calculated allowing the results reported here to be used once the lifetime of CFC-11 has been reassessed.

Appendix A

See Tables A1–A4 and Figs. A1–A3.

ACPD
13, 4221–4287, 2013

Appendix B

Correlation plots

In this section the correlation plots used in this work are shown. Species where the fit to the data failed are not included in these plots.

Appendix C

The mean vertical profiles of the species used in this study.

Acknowledgement. The ACE mission is supported primarily by the Canadian Space Agency. We would also like to thank the UK Natural Environment Research Council (NERC) and the National Centre for Earth Observation (NCEO) for financial support. With thanks to James Brooke for help with the seasonal variation.

References

Bernath, P. F.: Atmospheric chemistry experiment (ACE): analytical chemistry from orbit, TrAC Trends Anal. Chem., 25, 647–654, doi:10.1016/j.trac.2006.05.001, 2006.

Bernath, P. F., McElroy, C. T., Abrams, M. C., Boone, C. D., Butler, M., Camy-Peyret, C., Carleer, M., Clerbaux, C., Coheur, P. F., Colin, R., DeCola, P., DeMazière, M., Drummond, J. R., Dufour, D., Evans, W. F. J., Fast, H., Fussen, D., Gilbert, K., Jennings, D. E., Llewellyn, E. J., Lowe, R. P., Mahieu, E., McConnell, J. C., McHugh, M., McLeod, S. D., Michaud, R., Midwinter, C., Nassar, R., Nichitiu, F., Nowlan, C., Rinsland, C. P., Rochon, Y. J., Rowlands, N., Semeniuk, K., Simon, P., Skelton, R., Sloan, J. J., Soucy, M. A., Strong, K., Tremblay, P., Turnbull, D., Walker, K. A., Walkty, I., Wardle, D. A., Wehrle, V., Zander, R., and Zou, J.: Atmospheric Chemistry Experiment (ACE): mission overview, Geophys. Res. Lett., 32, L15S01, doi:10.1029/2005gl022386, 2005.

ACPD
13, 4221–4287, 2013

Boone, C. D., Nassar, R., Walker, K. A., Rochon, Y., McLeod, S. D., Rinsland, C. P., and Bernath, P. F.: Retrievals for the atmospheric chemistry experiment Fourier-transform spectrometer, Appl. Opt., 44, 7218–7231, 2005.

Brown, A. T., Chipperfield, M. P., Boone, C., Wilson, C., Walker, K. A., and Bernath, P. F.: Trends in atmospheric halogen containing gases since 2004, J. Quant. Spectrosc. Ra., 112, 2552–2566, doi:10.1016/j.jqsrt.2011.07.005, 2011.

Bujok, O., Tan, V., Klein, E., Nopper, R., Bauer, R., Engel, A., Gerhards, M.-T., Afchine, A., McKenna, D. S., Schmidt, U., Wienhold, F. G., and Fischer, H.: GHOST – a novel airborne gas chromatograph for in situ measurements of long-lived tracers in the lower stratosphere: method and applications, J. Atmos. Chem., 39, 37–64, doi:10.1023/a:1010789715871, 2001.

Cox, M. L., Sturrock, G. A., Fraser, P. J., Siems, S. T., Krummel, P. B., and O'Doherty, S.: Regional sources of methyl chloride, chloroform and dichloromethane identified from AGAGE observations at Cape Grim, Tasmania, 1998–2000, J. Atmos. Chem., 45, 79–99, doi:10.1023/a:1024022320985, 2003.

Cunnold, D. M., Weiss, R. F., Prinn, R. G., Hartley, D., Simmonds, P. G., Fraser, P. J., Miller, B., Alyea, F. N., and Porter, L.: GAGE/AGAGE measurements indicating reductions in global emissions of CCl_3F and CCl_2F_2 in 1992–1994, J. Geophys. Res., 102, 1259–1269, doi:10.1029/96jd02973, 1997.

Cunnold, D. M., Steele, L. P., Fraser, P. J., Simmonds, P. G., Prinn, R. G., Weiss, R. F., Porter, L. W., O'Doherty, S., Langenfelds, R. L., Krummel, P. B., Wang, H. J., Emmons, L., Tie, X. X., and Dlugokencky, E. J.: In situ measurements of atmospheric methane at GAGE/AGAGE sites during 1985–2000 and resulting source inferences, J. Geophys. Res., 107, 4225, doi:10.1029/2001jd001226, 2002.

Douglass, A. R., Stolarski, R. S., Schoeberl, M. R., Jackman, C. H., Gupta, M. L., Newman, P. A., Nielsen, J. E., and Fleming, E. L.: Relationship of loss, mean age of air and the distribution of CFCs to stratospheric circulation and implications for atmospheric lifetimes, J. Geophys. Res., 113, D14309, doi:10.1029/2007jd009575, 2008.

Irion, F. W., Gunson, M. R., Toon, G. C., Chang, A. Y., Eldering, A., Mahieu, E., Manney, G. L., Michelsen, H. A., Moyer, E. J., Newchurch, M. J., Osterman, G. B., Rinsland, C. P., Salawitch, R. J., Sen, B., Yung, Y. L., and Zander, R.: Atmospheric trace molecule spectroscopy (ATMOS) experiment version 3 data retrievals, Appl. Opt., 41, 6968–6979, 2002.

Johnston, H. S., Serang, O., and Podolske, J.: Instantaneous global nitrous oxide photochemical rates, J. Geophys. Res., 84, 5077–5082, doi:10.1029/JC084iC08p05077, 1979.
Ko, M. K., Newman, P. A., Reimann, S., and Strahan, S. E.: Lifetime of halogen source gases, in preperation, 2013.
Laube, J. C., Keil, A., Bönisch, H., Engel, A., Röckmann, T., Volk, C. M., and Sturges, W. T.: Observation-based assessment of stratospheric fractional release, lifetimes, and Ozone Depletion Potentials of ten important source gases, Atmos. Chem. Phys. Discuss., 12, 28525–28557, doi:10.5194/acpd-12-28525-2012, 2012.
Lide, D.: Handbook of chemistry and physics, in: Chemical Rubber Publishing Company, Florida, USA, 9–109, 1990.
Mäder, J. A., Staehelin, J., Peter, T., Brunner, D., Rieder, H. E., and Stahel, W. A.: Evidence for the effectiveness of the Montreal Protocol to protect the ozone layer, Atmos. Chem. Phys., 10, 12161–12171, doi:10.5194/acp-10-12161-2010, 2010.
Minschwaner, K., Carver, R. W., Briegleb, B. P., and Roche, A. E.: Infrared radiative forcing and atmospheric lifetimes of trace species based on observations from UARS, J. Geophys. Res., 103, 23243–23253, doi:10.1029/98jd02116, 1998.
Montzka, S. A., Reimann, S., (Coordinating Lead Authors), Engel , A., Krüger, K., O'Doherty, S., Sturges, W. T., Blake, D., Dorf, M., Fraser, P., Froidevaux, L., Jucks, K., Kreher, K., Kurylo, M. J., Mellouki, A., Miller, J., Nielsen, O.-J., Orkin, V. L., Prinn, R. G., Rhew, R., Santee, M. L., Stohl, A., and Verdonik, D.: Ozone-Depleting Substances (ODSs) and Related Chemicals, Chapt. 1 in Scientific Assessment of Ozone Depletion: 2010, Global Ozone Research and Monitoring Project – Report No. 52, World Meteorological Organization, Geneva, Switzerland, 2011.
Plumb, R. A.: A tropical pipe model of stratospheric transport, J. Geophys. Res., 101, 3957–3972, doi:10.1029/95jd03002, 1996.
Plumb, R. A.: Stratospheric transport, J. Meteorol. Soc. Japan, 80, 793–809, 2002.
Plumb, R. A.: Tracer interrelationships in the stratosphere, Rev. Geophys., 45, RG4005, doi:10.1029/2005rg000179, 2007.
Plumb, R. A. and Ko, M. K. W.: Interrelationships between mixing ratios of long-lived stratospheric constituents, J. Geophys. Res., 97, 10145–10156, doi:10.1029/92jd00450, 1992.
Prinn, R., Cunnold, D., Rasmussen, R., Simmonds, P., Alyea, F., Crawford, A., Fraser, P., and Rosen, R.: Atmospheric emissions and trends of nitrous oxide deduced from 10 years

ACPD
13, 4221–4287, 2013

Title Page
Abstract | Introduction
Conclusions | References
Tables | Figures
◀| |▶
◀ ▶
Back | Close
Full Screen / Esc
Printer-friendly Version
Interactive Discussion

of ALE;GAGE data, J. Geophys. Res., 95, 18369–18385, doi:10.1029/JD095iD11p18369, 1990.

Prinn, R. G., Zander, R., (Coordinating Lead Authors), Cunnold, D. M., Elkins, J. W., Engel, A., Fraser, P. J., Gunson, M. R., Ko, M. K. W., Mahieu, E., Midgley, P. M., Russell III, J. M., Volk, C. M., and Weis, R. F.: Long-Lived Ozone-Related Compounds, Chapter 1 in Scientific Assessment of Ozone Depletion: 1998, Global Ozone Research and Monitoring Project, Report No. 52, World Meteorological Organization, Geneva, Switzerland, 1999.

Prinn, R. G., Weiss, R. F., Fraser, P. J., Simmonds, P. G., Cunnold, D. M., Alyea, F. N., O'Doherty, S., Salameh, P., Miller, B. R., Huang, J., Wang, R. H. J., Hartley, D. E., Harth, C., Steele, L. P., Sturrock, G., Midgley, P. M., and McCulloch, A.: A history of chemically and radiatively important gases in air deduced from ALE/GAGE/AGAGE, J. Geophys. Res., 105, 17751–17792, doi:10.1029/2000jd900141, 2000.

Prinn, R. G., Huang, J., Weiss, R. F., Cunnold, D. M., Fraser, P. J., Simmonds, P. G., McCulloch, A., Harth, C., Salameh, P., O'Doherty, S., Wang, R. H. J., Porter, L., and Miller, B. R.: Evidence for substantial variations of atmospheric hydroxyl radicals in the past two decades, Science, 292, 1882–1888, doi:10.1126/science.1058673, 2001.

Rigby, M., Prinn, R. G., Fraser, P. J., Simmonds, P. G., Langenfelds, R. L., Huang, J., Cunnold, D. M., Steele, L. P., Krummel, P. B., Weiss, R. F., O'Doherty, S., Salameh, P. K., Wang, H. J., Harth, C. M., Mühle, J., and Porter, L. W.: Renewed growth of atmospheric methane, Geophys. Res. Lett., 35, L22805, doi:10.1029/2008gl036037, 2008.

Simmonds, P. G., Cunnold, D. M., Weiss, R. F., Prinn, R. G., Fraser, P. J., McCulloch, A., Alyea, F. N., and O'Doherty, S.: Global trends and emission estimates of CCl_4 from in situ background observations from July 1978 to June 1996, J. Geophys. Res., 103, 16017–16027, doi:10.1029/98jd01022, 1998.

Simmonds, P., Derwent, R., Manning, A., Fraser, P., Krummel, P., O'Doherty, S., Prinn, R., Cunnold, D., Miller, B., Wang, H., Ryall, D., Porter, L., Weiss, R., and Salameh, P.: AGAGE observations of methyl bromide and methyl chloride at Mace Head, Ireland, and Cape Grim, Tasmania, 1998–2001, J. Atmos. Chem., 47, 243–269, doi:10.1023/B:JOCH.0000021136.52340.9c, 2004.

Solomon, S., Qin, D., Manning, M., Alley, R. B., Berntsen, T., Bindoff, N. L., Chen, Z., Chidthaisong, A., Gregory, J. M., Hegerl, G. C., Heimann, M., Hewitson, B., Hoskins, B. J., Joos, F., Jouzel, J., Kattsov, V., Lohmann, U., Matsuno, T., Molina, M., Nicholls, N., Overpeck, J., Raga, G., Ramaswamy, V., Ren, J., Rusticucci, M., Somerville, R., Stocker, T. F., Whetton, P., Wood, R. A., Wratt, D: Climate Change 2007: The Physical Science Basis. Contribution of Working Group I to the Fourth Assessment Report of the Intergovernmental Panel on Climate Change, Cambridge University Press, Cambridge, 2007.

UNEP: Handbook for the Montreal Protocol on Substances that Deplete the Ozone Layer 8 edn., Secretariat for The Vienna Convention for the Protection of the Ozone Layer & The Montreal Protocol on Substances that Deplete the Ozone Layer, Nairobi, Kenya, 2009.

Velders, G. J. M., Andersen, S. O., Daniel, J. S., Fahey, D. W., and McFarland, M.: The importance of the Montreal Protocol in protecting climate, Proc. Natl. Acad. Sci. USA, 104, 4814–4819, doi:10.1073/pnas.0610328104, 2007.

Volk, C. M., Elkins, J. W., Fahey, D. W., Dutton, G. S., Gilligan, J. M., Loewenstein, M., Podolske, J. R., Chan, K. R., and Gunson, M. R.: Evaluation of source gas lifetimes from stratospheric observations, J. Geophys. Res., 102, 25543–25564, doi:10.1029/97jd02215, 1997.

ACPD
13, 4221–4287, 2013

Stratospheric lifetimes of CFC-12, CCl_4, CH_4, CH_3Cl and N_2O

A. T. Brown et al.

Table 1. The slope of the age of air against the volume mixing ratio of CFC-11 at the tropopause.

	Age of Air $ppt\,yr^{-1}$
2005	-21.3 ± 4.6
2006	-21.1 ± 4.6
2007	-20.9 ± 4.6
2008	-20.7 ± 4.6
2009	-20.6 ± 4.6
2010	-20.5 ± 4.6

ACPD
13, 4221–4287, 2013

Table 2. The effective linear growth rates (γ_0) in % yr^{-1} of CFC-11, CFC-12, CCl_4, CH_4, CH_3Cl and N_2O.

	CFC-11	CFC-12	CH_3Cl
2005	−0.853 ± 0.019	−0.181 ± 0.01	1.661 ± 0.556
2006	−0.92 ± 0.022	−0.286 ± 0.012	−0.428 ± 0.712
2007	−0.905 ± 0.023	−0.383 ± 0.011	0.665 ± 0.469
2008	−0.831 ± 0.026	−0.452 ± 0.013	0.862 ± 0.326
2009	−0.727 ± 0.019	−0.486 ± 0.012	−0.144 ± 0.291
2010	−0.718 ± 0.018	−0.478 ± 0.009	−0.384 ± 0.245
	CCl_4	N_2O	CH_4
2005	−0.933 ± 0.024	0.205 ± 0.007	0.003 ± 0.043
2006	−0.944 ± 0.026	0.212 ± 0.008	−0.034 ± 0.039
2007	−1.133 ± 0.032	0.217 ± 0.011	0.17 ± 0.059
2008	−1.305 ± 0.028	0.262 ± 0.008	0.477 ± 0.045
2009	−1.451 ± 0.023	0.257 ± 0.009	0.444 ± 0.046
2010	−1.479 ± 0.027	0.262 ± 0.009	0.328 ± 0.047

Table 3. The calculated lifetimes of CFC-12, CCl_4, CH_4, CH_3Cl and N_2O using a CFC-11 lifetime of 45 yr. NHS = Northern Hemisphere Summer, NHW = Northern Hemisphere Winter, SHS = Southern Hemisphere Winter, SHW = Southern Hemisphere Winter.

	Bin	CFC-12	CH_3Cl	CCl_4	N_2O	CH_4
2005	NHW	107 + (−)11(9)	123 + (−)156(43)	34 + (−)4(3)	–	–
	SHW	87 + (−)27(17)	34 + (−)170(16)	62 + (−)107(24)	91 + (−)12(10)	81 + (−)27(16)
2006	NHS	121 + (−)11(9)	–	49 + (−)20(11)	177 + (−)30(22)	218 + (−)42(31)
	NHW	89 + (−)15(12)	48 + (−)12(8)	24 + (−)3(2)	–	196 + (−)97(49)
	SHS	82 + (−)7(6)	35 + (−)7(5)	43 + (−)9(7)	153 + (−)44(28)	308 + (−)135(73)
	SHW	132 + (−)23(18)	123 + (−)149(44)	46 + (−)4(4)	85 + (−)10(8)	157 + (−)17(14)
2007	NHS	131 + (−)16(13)	–	23 + (−)2(2)	–	241 + (−)35(26)
	NHW	132 + (−)14(12)	–	41 + (−)8(6)	180 + (−)150(56)	221 + (−)72(44)
	SHS	90 + (−)14(11)	65 + (−)105(25)	46 + (−)27(13)	118 + (−)21(16)	231 + (−)50(35)
	SHW	95 + (−)8(7)	83 + (−)72(26)	35 + (−)3(3)	99 + (−)13(10)	136 + (−)19(15)
2008	NHS	96 + (−)6(6)	116 + (−)103(37)	30 + (−)2(2)	–	–
	NHW	87 + (−)9(8)	72 + (−)40(19)	28 + (−)2(2)	164 + (−)24(19)	202 + (−)32(22)
	SHS	121 + (−)15(12)	94 + (−)53(25)	32 + (−)4(3)	173 + (−)30(22)	–
	SHW	121 + (−)30(20)	83 + (−)91(29)	40 + (−)3(2)	113 + (−)16(12)	218 + (−)34(23)
2009	NHS	104 + (−)13(11)	–	17 + (−)4(3)	208 + (−)143(60)	204 + (−)57(36)
	NHW	–	–	–	–	–
	SHS	84 + (−)29(18)	–	28 + (−)8(5)	66 + (−)12(9)	89 + (−)41(21)
	SHW	109 + (−)7(7)	36 + (−)14(8)	36 + (−)9(6)	94 + (−)8(7)	222 + (−)30(21)
2010	NHS	150 + (−)11(10)	–	28 + (−)3(3)	185 + (−)54(34)	159 + (−)35(24)
	NHW	123 + (−)19(15)	49 + (−)29(13)	28 + (−)2(2)	95 + (−)17(13)	123 + (−)11(9)
	SHS	96 + (−)12(10)	70 + (−)108(27)	40 + (−)10(7)	120 + (−)23(17)	302 + (−)159(77)
	SHW	87 + (−)14(11)	54 + (−)51(18)	85 + (−)59(25)	100 + (−)11(9)	211 + (−)43(30)

ACPD
13, 4221–4287, 2013

Table 4. The mean lifetimes of CFC-12, CCl_4, CH_4, CH_3Cl and N_2O using a CFC-11 lifetime of 45 yr. NHS = Northern Hemisphere Summer, NHW = Northern Hemisphere Winter, SHS = Southern Hemisphere Winter, SHW = Southern Hemisphere Winter, NH = Northern Hemisphere, SH = Southern Hemisphere.

	CFC-12	CH_3Cl	CCl_4	N_2O	CH_4
NHS	123 + (−)31(21)	116 + (−)102(37)	28 + (−)8(5)	182 + (−)12(10)	218 + (−)43(31)
NHW	111 + (−)25(17)	66 + (−)45(19)	30 + (−)5(4)	146 + (−)65(34)	161 + (−)69(37)
SHS	97 + (−)21(15)	58 + (−)68(20)	36 + (−)7(5)	136 + (−)68(34)	253 + (−)139(66)
SHW	106 + (−)15(12)	75 + (−)86(26)	42 + (−)8(6)	97 + (−)9(8)	189 + (−)62(37)
NH	119 + (−)29(19)	74 + (−)62(23)	29 + (−)6(4)	163 + (−)53(32)	188 + (−)76(42)
SH	103 + (−)18(13)	66 + (−)72(23)	41 + (−)9(6)	109 + (−)34(21)	200 + (−)78(44)
Summer	116 + (−)32(21)	69 + (−)103(26)	31 + (−)9(6)	153 + (−)69(36)	229 + (−)67(42)
Winter	108 + (−)19(14)	70 + (−)55(21)	36 + (−)11(7)	108 + (−)31(20)	179 + (−)65(38)
All data	113 + (−)26(18)	69 + (−)65(23)	35 + (−)11(7)	123 + (−)53(28)	195 + (−)75(42)

ACPD
13, 4221–4287, 2013

Table 5. The ratio of $\tau_\chi/\tau_{CFC\text{-}11}$ for CFC-12, CCl_4, CH_4, CH_3Cl and N_2O.

Trace gas	Lifetime ratio to CFC-11
CFC-12	2.5 + (–)0.57(0.39)
CH_3Cl	1.54 + (–)1.44(0.5)
CCl_4	0.77 + (–)0.25(0.15)
N_2O	2.74 + (–)1.18(0.63)
CH_4	4.33 + (–)1.66(0.94)

ACPD
13, 4221–4287, 2013

Table A1. The slopes of the correlations of CFC-12, CCl_4, CH_4, CH_3Cl and N_2O with CFC-11, extrapolated to the tropopause. NHS = Northern Hemisphere Summer, NHW = Northern Hemisphere Winter, SHS = Southern Hemisphere Winter, SHW = Southern Hemisphere Winter. Data with errors greater than the correlations have been removed.

	Bin	CFC-12	CH_3Cl	CCl_4	N_2O	CH_4
2005	NHW	0.96 ± 0.08	1.21 ± 0.37	0.6 ± 0.07	–	–
	SHW	1.19 ± 0.29	3.16 ± 2.24	0.31 ± 0.22	716.81 ± 75.47	4403.1 ± 1080.64
2006	NHS	0.82 ± 0.06	–	0.41 ± 0.13	386.3 ± 47.25	1609.02 ± 257.51
	NHW	1.14 ± 0.17	1.91 ± 0.37	0.89 ± 0.1	–	1794.21 ± 599.76
	SHS	1.25 ± 0.1	2.68 ± 0.43	0.47 ± 0.09	441.96 ± 89.48	1130.28 ± 348.86
	SHW	0.75 ± 0.12	0.68 ± 0.39	0.44 ± 0.03	764.16 ± 66.93	2240.74 ± 193.1
2007	NHS	0.73 ± 0.08	–	0.91 ± 0.07	–	1631.25 ± 154.93
	NHW	0.72 ± 0.07	–	0.48 ± 0.08	384.17 ± 158.75	1768.92 ± 385.62
	SHS	1.1 ± 0.16	1.71 ± 0.93	0.42 ± 0.18	568.32 ± 76.45	1694.7 ± 255.45
	SHW	1.04 ± 0.08	1.38 ± 0.52	0.57 ± 0.05	668.52 ± 63.26	2775.14 ± 288.66
2008	NHS	1.02 ± 0.06	1.08 ± 0.38	0.67 ± 0.05	–	–
	NHW	1.14 ± 0.11	1.6 ± 0.47	0.71 ± 0.04	425.58 ± 43.92	2180.86 ± 171.34
	SHS	0.79 ± 0.09	1.29 ± 0.36	0.61 ± 0.06	405.89 ± 48.77	–
	SHW	0.78 ± 0.17	1.43 ± 0.61	0.48 ± 0.03	599.92 ± 61.47	2049.66 ± 145.78
2009	NHS	0.92 ± 0.11	–	1.24 ± 0.26	342.99 ± 122.16	2139.97 ± 351.11
	NHW	–	–	–	–	–
	SHS	1.17 ± 0.34	–	0.72 ± 0.18	992.12 ± 144.53	4408.87 ± 1253.71
	SHW	0.87 ± 0.05	2.72 ± 0.75	0.54 ± 0.12	710.83 ± 43.07	1997.24 ± 111.75
2010	NHS	0.61 ± 0.04	–	0.71 ± 0.08	386.97 ± 74.89	2566.37 ± 387.05
	NHW	0.76 ± 0.11	1.95 ± 0.76	0.72 ± 0.04	716.72 ± 98.31	3244.25 ± 157.55
	SHS	1.01 ± 0.12	1.34 ± 0.87	0.47 ± 0.11	572.71 ± 81.13	1485.76 ± 396.57
	SHW	1.14 ± 0.17	1.77 ± 0.92	0.18 ± 0.1	680.5 ± 55.37	2003.68 ± 256.47

Table A2. The mean volume mixing ratio at the tropopause (σ_0). NHS = Northern Hemisphere Summer, NHW = Northern Hemisphere Winter, SHS = Southern Hemisphere Summer, SHW = Southern Hemisphere Winter.

	CFC-11	CFC-12	CH_3Cl	CCl_4	N_2O	CH_4
2005	245.24 ± 3.14	515.63 ± 4.88	575.6 ± 9.86	106.33 ± 3.14	315.3 ± 2	1747.5 ± 33.4
2006	240.9 ± 3	512.54 ± 7.82	586.4 ± 27.78	106.83 ± 7.34	315.7 ± 2.5	1755.8 ± 36.2
2007	238.23 ± 1.72	510.97 ± 4.19	612.36 ± 25.76	106.59 ± 7.8	316.5 ± 0.7	1762.6 ± 34.9
2008	237.84 ± 3.03	509.52 ± 5.94	571.52 ± 39.13	104.51 ± 6.89	317.4 ± 2	1765.5 ± 36.1
2009	235.54 ± 4.54	510.17 ± 7.25	596.21 ± 11.75	105.45 ± 9.15	317.7 ± 2.2	1770 ± 26.2
2010	232 ± 2.72	503.36 ± 6.83	572.45 ± 23.35	101.29 ± 7.47	317.3 ± 4.4	1770.5 ± 38.2

ACPD
13, 4221–4287, 2013

Stratospheric lifetimes of CFC-12, CCl_4, CH_4, CH_3Cl and N_2O

A. T. Brown et al.

Title Page
Abstract | Introduction
Conclusions | References
Tables | Figures
◀| |▶
◀ ▶
Back | Close
Full Screen / Esc
Printer-friendly Version
Interactive Discussion

Table A3. The corrected slopes of the correlations of CFC-12, CCl_4, CH_4, CH_3Cl and N_2O with CFC-11, extrapolated to the tropopause. NHS = Northern Hemisphere Summer, NHW = Northern Hemisphere Winter, SHS = Southern Hemisphere Summer, SHW = Southern Hemisphere Winter.

	Bin	CFC-12	CH_3Cl	CCl_4
2005	NHW	0.93 + (−)0.08(0.08)	0.74 + (−)0.4(0.41)	0.59 + (−)0.06(0.06)
	SHW	1.15 + (−)0.27(0.27)	2.63 + (−)2.18(2.19)	0.32 + (−)0.2(0.2)
2006	NHS	0.82 + (−)0.06(0.06)	–	0.41 + (−)0.12(0.12)
	NHW	1.11 + (−)0.16(0.16)	1.86 + (−)0.37(0.37)	0.85 + (−)0.09(0.09)
	SHS	1.21 + (−)0.09(0.09)	2.56 + (−)0.42(0.42)	0.47 + (−)0.08(0.08)
	SHW	0.75 + (−)0.11(0.11)	0.73 + (−)0.4(0.4)	0.44 + (−)0.03(0.03)
2007	NHS	0.76 + (−)0.08(0.08)	–	0.87 + (−)0.07(0.07)
	NHW	0.75 + (−)0.07(0.07)	–	0.48 + (−)0.08(0.08)
	SHS	1.1 + (−)0.14(0.14)	1.43 + (−)0.88(0.88)	0.43 + (−)0.16(0.16)
	SHW	1.04 + (−)0.08(0.08)	1.11 + (−)0.51(0.52)	0.57 + (−)0.05(0.05)
2008	NHS	1.04 + (−)0.05(0.05)	0.81 + (−)0.37(0.38)	0.67 + (−)0.04(0.04)
	NHW	1.15 + (−)0.1(0.1)	1.3 + (−)0.45(0.46)	0.7 + (−)0.03(0.03)
	SHS	0.83 + (−)0.09(0.09)	1 + (−)0.35(0.36)	0.61 + (−)0.06(0.06)
	SHW	0.82 + (−)0.16(0.16)	1.13 + (−)0.59(0.59)	0.49 + (−)0.02(0.02)
2009	NHS	0.97 + (−)0.1(0.1)	–	1.19 + (−)0.23(0.23)
	NHW	–	–	–
	SHS	1.2 + (−)0.31(0.31)	–	0.72 + (−)0.17(0.17)
	SHW	0.92 + (−)0.04(0.05)	2.58 + (−)0.71(0.71)	0.56 + (−)0.11(0.11)
2010	NHS	0.67 + (−)0.04(0.04)	–	0.71 + (−)0.07(0.07)
	NHW	0.82 + (−)0.11(0.11)	1.92 + (−)0.71(0.71)	0.72 + (−)0.04(0.04)
	SHS	1.05 + (−)0.11(0.11)	1.35 + (−)0.82(0.82)	0.5 + (−)0.1(0.1)
	SHW	1.17 + (−)0.16(0.16)	1.75 + (−)0.86(0.86)	0.23 + (−)0.1(0.1)

	Bin	N_2O	CH_4
2005	NHW	–	–
	SHW	641.7 + (−)72.5(74.6)	4093 + (−)1008.3(1011.1)
2006	NHS	330 + (−)45.5(47.2)	1514.5 + (−)241.2(242.5)
	NHW	–	1685.8 + (−)556.3(556.9)
	SHS	381.8 + (−)84.3(85.3)	1071.7 + (−)324.4(324.8)
	SHW	681.7 + (−)65.1(67.9)	2098.9 + (−)184.5(187.9)
2007	NHS	–	1385.4 + (−)159.1(168.1)
	NHW	327.5 + (−)148.5(149)	1513.6 + (−)365.6(369.9)
	SHS	499.2 + (−)72.9(74.6)	1444.5 + (−)247.3(253.5)
	SHW	592.6 + (−)61.4(63.9)	2450.4 + (−)281.3(291.2)
2008	NHS	–	–
	NHW	361.7 + (−)43.3(45.7)	1674.3 + (−)193.2(222.5)
	SHS	343.2 + (−)47.6(49.6)	–
	SHW	525.2 + (−)60(62.5)	1550.5 + (−)172.3(203.4)
2009	NHS	287 + (−)116.1(116.8)	1671.6 + (−)348.4(363.6)
	NHW	–	–
	SHS	901.2 + (−)138.5(140.3)	3828.4 + (−)1199.3(1207.5)
	SHW	635 + (−)44.2(47.9)	1535.9 + (−)144.3(176.8)
2010	NHS	328.1 + (−)72(73.3)	2166.2 + (−)378.5(389.8)
	NHW	640.6 + (−)94.8(96.6)	2809.5 + (−)180.4(208.2)
	SHS	504.1 + (−)78.3(80.1)	1140.6 + (−)384.2(391.7)
	SHW	606.3 + (−)55.1(58)	1632.1 + (−)257.4(270.9)

ACPD
13, 4221–4287, 2013

Table A4. Mean atmospheric volume mixing ratio ($\overline{\sigma}$). NHS = Northern Hemisphere Summer, NHW = Northern Hemisphere Winter, SHS = Southern Hemisphere Winter, SHW = Southern Hemisphere Winter.

	CFC-11	CFC-12	CH_3Cl	CCl_4	N_2O	CH_4
2005	230.31 ± 5.74	508.14 ± 13.75	463.23 ± 12.83	103.28 ± 2.67	299 ± 8.0	1689 ± 44.9
2006	230.27 ± 6.22	505.64 ± 13.67	458.31 ± 3.64	103.56 ± 2.87	298.1 ± 8.0	1689.6 ± 44.9
2007	227.95 ± 6.20	502.6 ± 13.63	468.97 ± 13.08	100.25 ± 2.77	297.9 ± 7.9	1690.7 ± 44.8
2008	225.61 ± 6.07	500.15 ± 13.51	470.97 ± 13.15	99.2 ± 2.72	296.9 ± 7.9	1695.8 ± 45.0
2009	222.6 ± 6.04	497.68 ± 13.48	456.11 ± 12.73	98.48 ± 2.73	295.5 ± 7.9	1683.4 ± 44.7
2010	221.03 ± 6.00	495.96 ± 13.39	462.15 ± 12.77	97.52 ± 2.67	298.1 ± 7.9	1694.4 ± 44.8

ACPD
13, 4221–4287, 2013

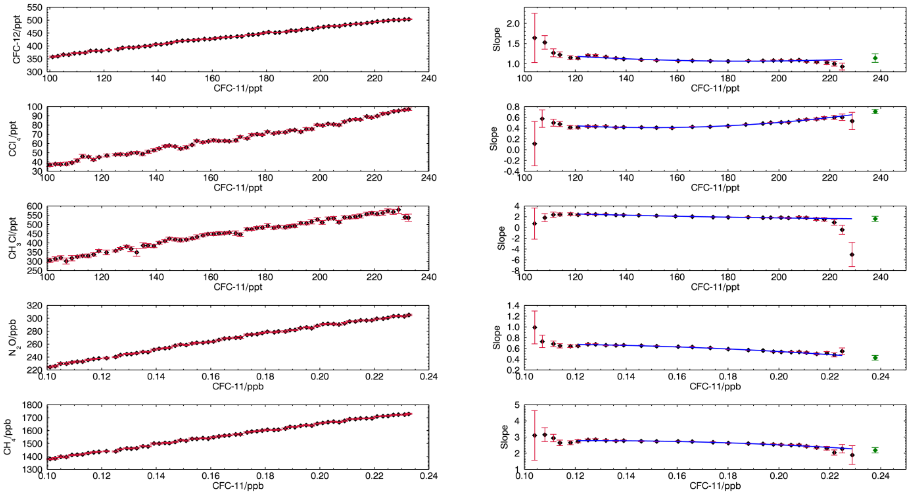

Fig. 1. Correlations between the volume mixing ratios of CFC-12, CCl_4, CH_4, CH_3Cl and N_2O and CFC-11 for the data from the Northern Hemisphere during the stratospheric winter of 2008. Left panels: the mean correlation curves. Each point represents the mean of the VMR, of both CFC-11 and CFC-12, in a window of 2 ppt of CFC-11. The error on these points is the standard deviation of the data within each 2 ppt window. Right panels: The local slope of data in an 80 ppt of CFC-11 window. The error on the points is the fitting error of this fit. The blue line is a second degree polynomial fit to the local slopes. The green point is the extrapolated slope at the tropopause.

ACPD
13, 4221–4287, 2013

Stratospheric lifetimes of CFC-12, CCl_4, CH_4, CH_3Cl and N_2O

A. T. Brown et al.

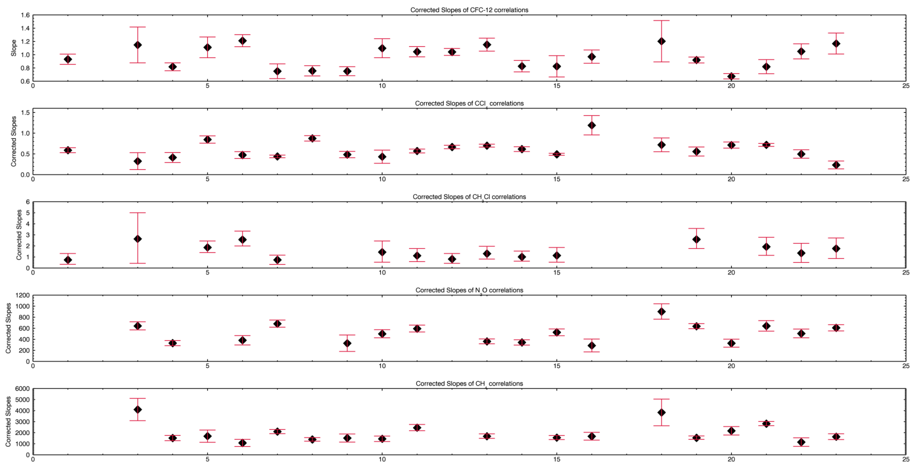

Fig. A1. A graphical representation of the slopes of the various correlations with CFC-11. The data is presented in the same order as it appears in Table 1 above.

ACPD
13, 4221–4287, 2013

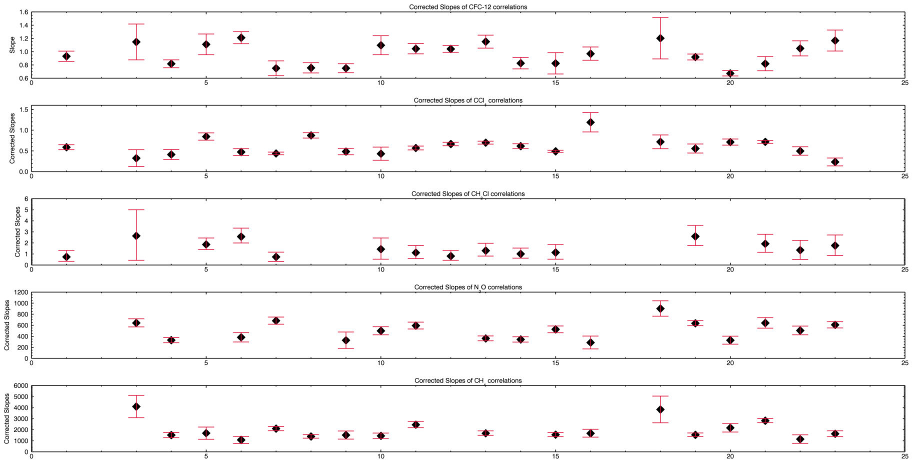

Fig. A2. A graphical representation of the corrected slopes of the various correlations with CFC-11. The data is presented in the same order as it appears in Table 3 above.

ACPD
13, 4221–4287, 2013

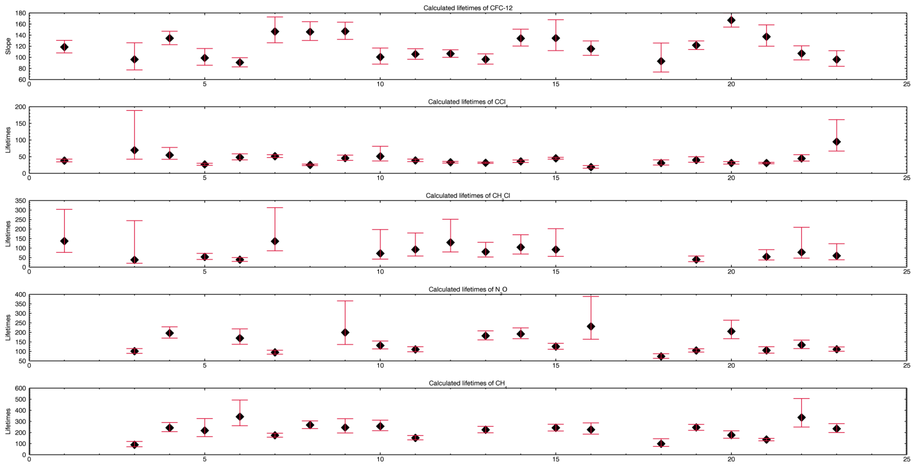

Fig. A3. A graphical representation of the lifetimes of CFC-12, CCl_4, CH_3Cl, N_2O and CH_4 calculated using a CFC-11 of 50 yr. The data is presented in the same order as it appears in the main paper.

ACPD
13, 4221–4287, 2013

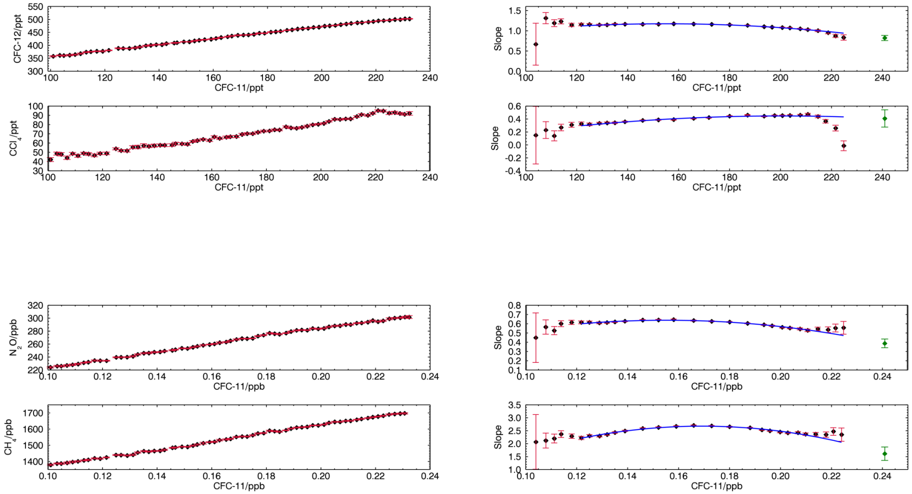

Fig. B1. Correlations between the volume mixing ratios of CFC-12, CCl_4, CH_4, and N_2O and CFC-11 for the data from the Northern Hemisphere during the stratospheric summer of 2006. Left panels: the mean correlation profile. Each point represents the mean of the VMR in a window of 2 ppt of CFC-11. The error on these points is the standard deviation of the data within each 2 ppt window. Right panels: the local slope of data in an 80 ppt of CFC-11 window. The error on the points is the fitting error of this fit. The blue line is a second degree polynomial fit to the local slopes. The green point is the extrapolated slope at the tropopause.

ACPD
13, 4221–4287, 2013

Stratospheric lifetimes of CFC-12, CCl_4, CH_4, CH_3Cl and N_2O

A. T. Brown et al.

Discussion Paper | Discussion Paper | Discussion Paper | Discussion Paper |

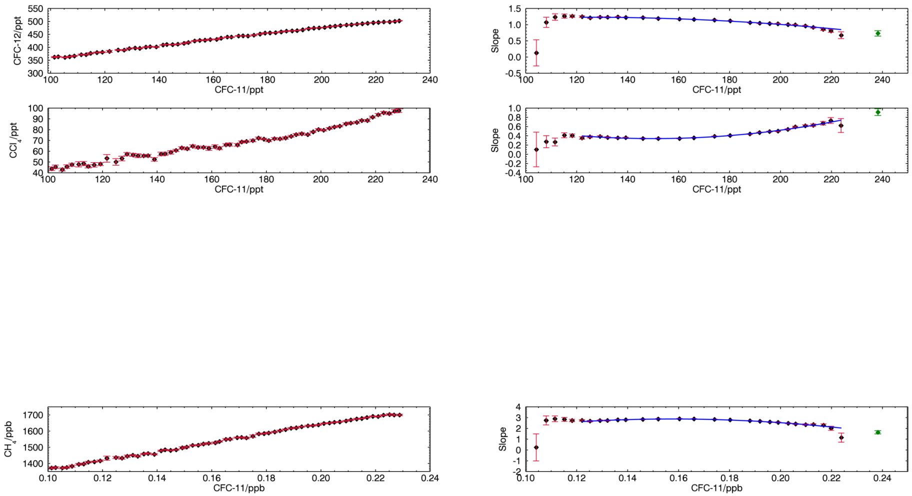

Fig. B2. Correlations between the volume mixing ratios of CFC-12, CCl_4, and CH_4 and CFC-11 for the data from the Northern Hemisphere during the stratospheric summer of 2007. Left panels: the mean correlation profile. Each point represents the mean of the VMR in a window of 2 ppt of CFC-11. The error on these points is the standard deviation of the data within each 2 ppt window. Right panels: the local slope of data in an 80 ppt of CFC-11 window. The error on the points is the fitting error of this fit. The blue line is a second degree polynomial fit to the local slopes. The green point is the extrapolated slope at the tropopause.

ACPD

13, 4221–4287, 2013

Stratospheric lifetimes of CFC-12, CCl_4, CH_4, CH_3Cl and N_2O

A. T. Brown et al.

Title Page
Abstract | Introduction
Conclusions | References
Tables | Figures
◂| |▸
◂ ▸
Back | Close
Full Screen / Esc
Printer-friendly Version
Interactive Discussion

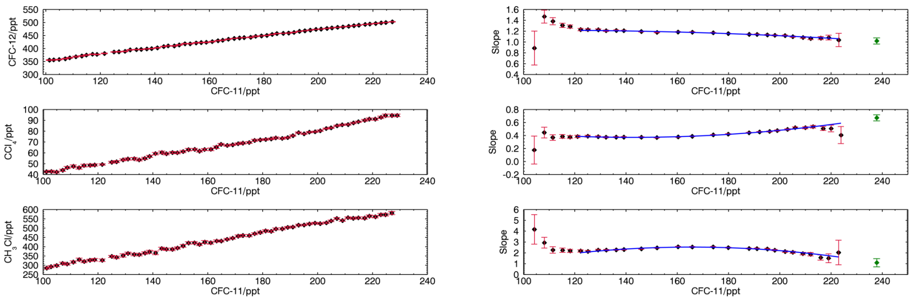

Fig. B3. Correlations between the volume mixing ratios of CFC-12, CCl_4, and CH_3Cl and CFC-11 for the data from the Northern Hemisphere during the stratospheric summer of 2008. Left panels: the mean correlation profile. Each point represents the mean of the VMR in a window of 2 ppt of CFC-11. The error on these points is the standard deviation of the data within each 2 ppt window. Right panels: the local slope of data in an 80 ppt of CFC-11 window. The error on the points is the fitting error of this fit. The blue line is a second degree polynomial fit to the local slopes. The green point is the extrapolated slope at the tropopause.

ACPD
13, 4221–4287, 2013

Stratospheric lifetimes of CFC-12, CCl_4, CH_4, CH_3Cl and N_2O

A. T. Brown et al.

Title Page
Abstract | Introduction
Conclusions | References
Tables | Figures
◀| |▶
◀ ▶
Back | Close
Full Screen / Esc
Printer-friendly Version
Interactive Discussion

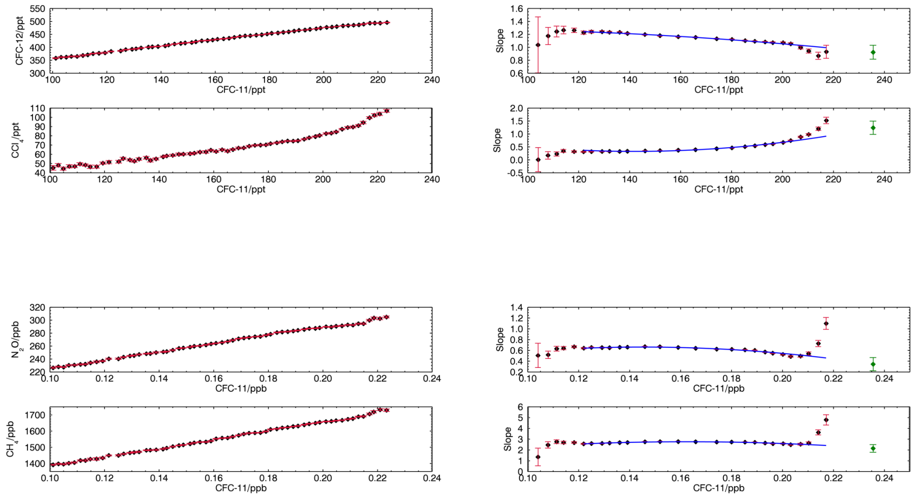

Fig. B4. Correlations between the volume mixing ratios of CFC-12, CCl_4, CH_4 and N_2O and CFC-11 for the data from the Northern Hemisphere during the stratospheric summer of 2009. Left panels: the mean correlation profile. Each point represents the mean of the VMR in a window of 2 ppt of CFC-11. The error on these points is the standard deviation of the data within each 2 ppt window. Right panels: the local slope of data in an 80 ppt of CFC-11 window. The error on the points is the fitting error of this fit. The blue line is a second degree polynomial fit to the local slopes. The green point is the extrapolated slope at the tropopause.

ACPD
13, 4221–4287, 2013

Stratospheric lifetimes of CFC-12, CCl_4, CH_4, CH_3Cl and N_2O

A. T. Brown et al.

Title Page
Abstract | Introduction
Conclusions | References
Tables | Figures
◂◂ | ▸▸
◂ | ▸
Back | Close
Full Screen / Esc
Printer-friendly Version
Interactive Discussion

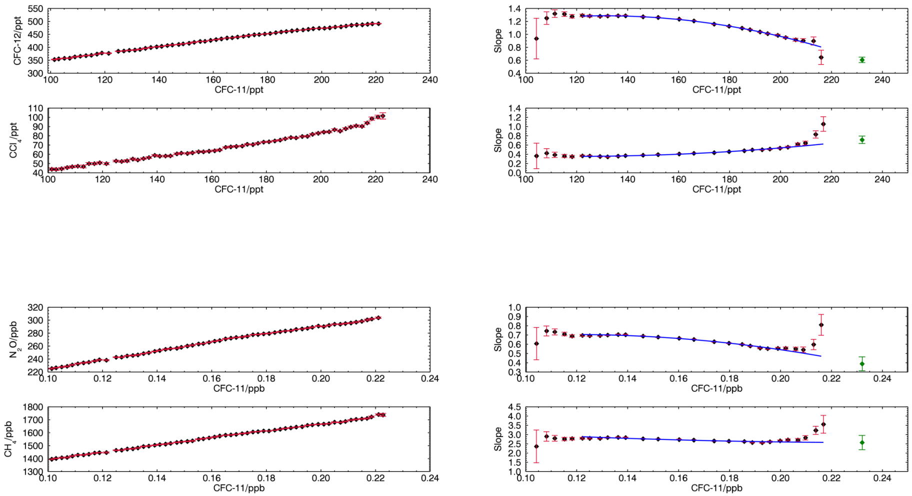

Fig. B5. Correlations between the volume mixing ratios of CFC-12, CCl_4, CH_4 and N_2O and CFC-11 for the data from the Northern Hemisphere during the stratospheric summer of 2010. Left panels: the mean correlation profile. Each point represents the mean of the VMR in a window of 2 ppt of CFC-11. The error on these points is the standard deviation of the data within each 2 ppt window. Right panels: the local slope of data in an 80 ppt of CFC-11 window. The error on the points is the fitting error of this fit. The blue line is a second degree polynomial fit to the local slopes. The green point is the extrapolated slope at the tropopause.

ACPD
13, 4221–4287, 2013

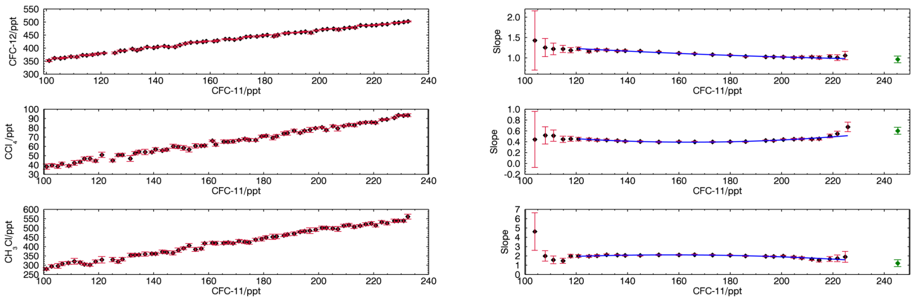

Fig. B6. Correlations between the volume mixing ratios of CFC-12, CCl_4 and CH_3Cl and CFC-11 for the data from the Northern Hemisphere during the stratospheric winter of 2005. Left panels: the mean correlation profile. Each point represents the mean of the VMR in a window of 2 ppt of CFC-11. The error on these points is the standard deviation of the data within each 2 ppt window. Right panels: the local slope of data in an 80 ppt of CFC-11 window. The error on the points is the fitting error of this fit. The blue line is a second degree polynomial fit to the local slopes. The green point is the extrapolated slope at the tropopause.

ACPD

13, 4221–4287, 2013

Stratospheric lifetimes of CFC-12, CCl_4, CH_4, CH_3Cl and N_2O

A. T. Brown et al.

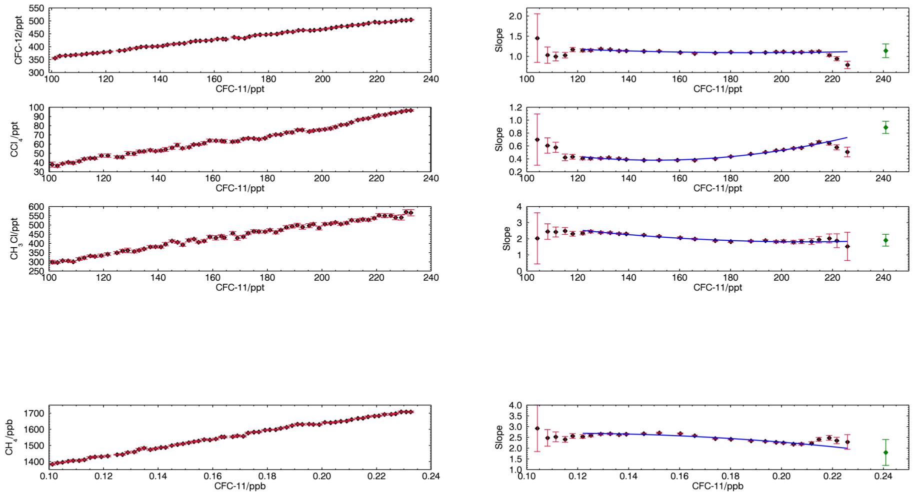

Fig. B7. Correlations between the volume mixing ratios of CFC-12, CCl_4, CH_4 and CH_3Cl and CFC-11 for the data from the Northern Hemisphere during the stratospheric winter of 2006. Left panels: the mean correlation profile. Each point represents the mean of the VMR in a window of 2 ppt of CFC-11. The error on these points is the standard deviation of the data within each 2 ppt window. Right panels: the local slope of data in an 80 ppt of CFC-11 window. The error on the points is the fitting error of this fit. The blue line is a second degree polynomial fit to the local slopes. The green point is the extrapolated slope at the tropopause.

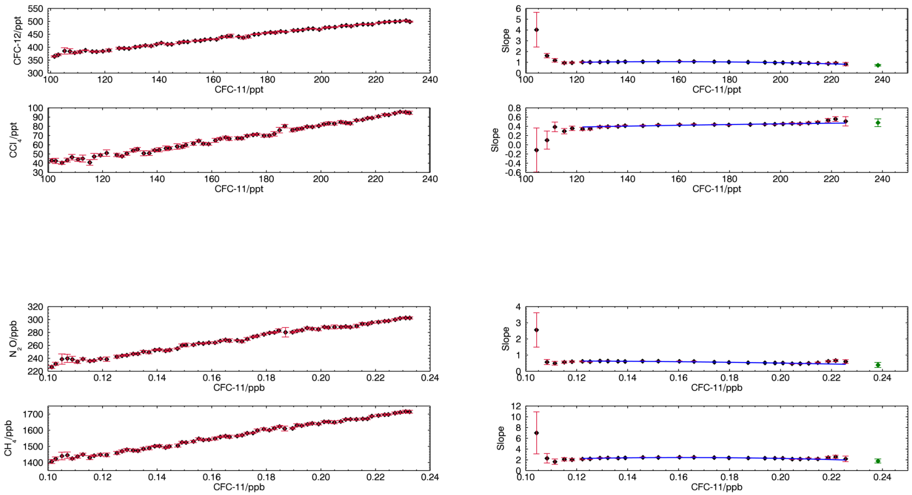

Fig. B8. Correlations between the volume mixing ratios of CFC-12, CCl_4, CH_4 and N_2O and CFC-11 for the data from the Northern Hemisphere during the stratospheric winter of 2007. Left panels: the mean correlation profile. Each point represents the mean of the VMR in a window of 2 ppt of CFC-11. The error on these points is the standard deviation of the data within each 2 ppt window. Right panels: the local slope of data in an 80 ppt of CFC-11 window. The error on the points is the fitting error of this fit. The blue line is a second degree polynomial fit to the local slopes. The green point is the extrapolated slope at the tropopause.

ACPD
13, 4221–4287, 2013

Stratospheric lifetimes of CFC-12, CCl_4, CH_4, CH_3Cl and N_2O

A. T. Brown et al.

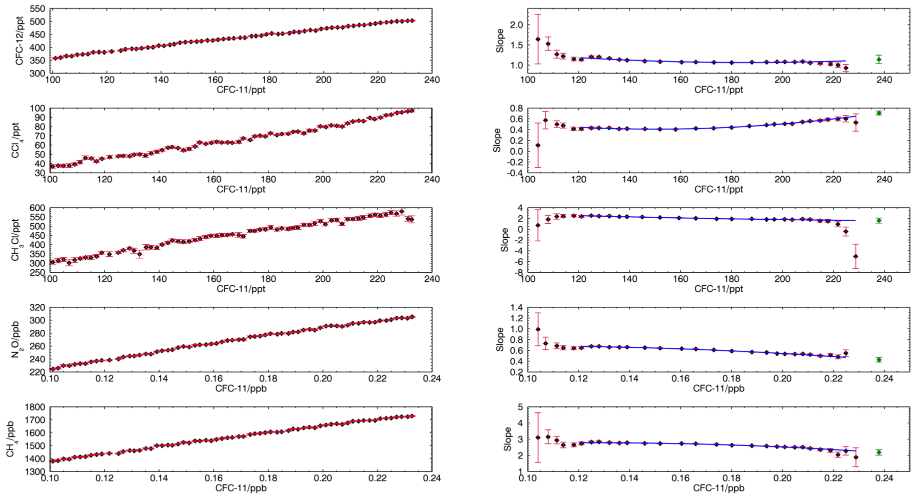

Fig. B9. Correlations between the volume mixing ratios of CFC-12, CCl_4, CH_4, CH_3Cl and N_2O and CFC-11 for the data from the Northern Hemisphere during the stratospheric winter of 2008. Left panels: the mean correlation profile. Each point represents the mean of the VMR in a window of 2 ppt of CFC-11. The error on these points is the standard deviation of the data within each 2 ppt window. Right panels: the local slope of data in an 80 ppt of CFC-11 window. The error on the points is the fitting error of this fit. The blue line is a second degree polynomial fit to the local slopes. The green point is the extrapolated slope at the tropopause.

ACPD
13, 4221–4287, 2013

Stratospheric lifetimes of CFC-12, CCl_4, CH_4, CH_3Cl and N_2O

A. T. Brown et al.

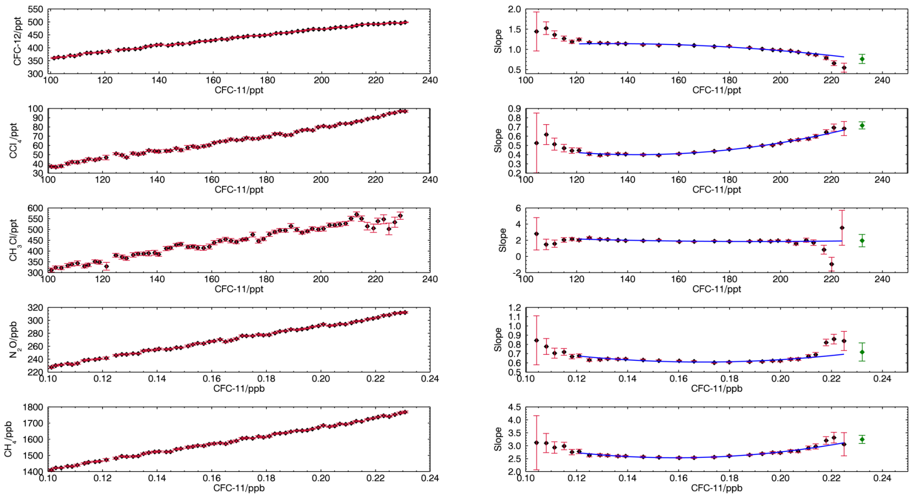

Fig. B10. Correlations between the volume mixing ratios of CFC-12, CCl_4, CH_4, CH_3Cl and N_2O and CFC-11 for the data from the Northern Hemisphere during the stratospheric winter of 2010. Left panels: the mean correlation profile. Each point represents the mean of the VMR in a window of 2 ppt of CFC-11. The error on these points is the standard deviation of the data within each 2 ppt window. Right panels: the local slope of data in an 80 ppt of CFC-11 window. The error on the points is the fitting error of this fit. The blue line is a second degree polynomial fit to the local slopes. The green point is the extrapolated slope at the tropopause.

ACPD
13, 4221–4287, 2013

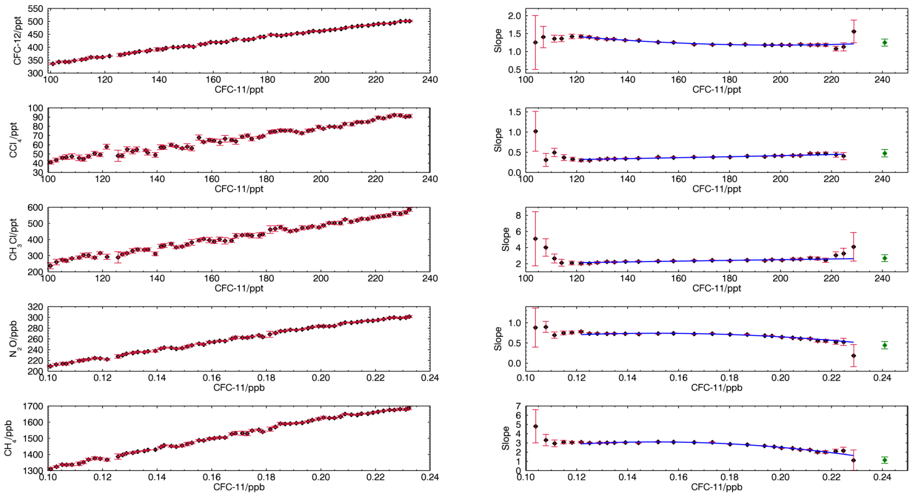

Fig. B11. Correlations between the volume mixing ratios of CFC-12, CCl_4, CH_4, CH_3Cl and N_2O and CFC-11 for the data from the Southern Hemisphere during the stratospheric summer of 2006. Left panels: the mean correlation profile. Each point represents the mean of the VMR in a window of 2 ppt of CFC-11. The error on these points is the standard deviation of the data within each 2 ppt window. Right panels: the local slope of data in an 80 ppt of CFC-11 window. The error on the points is the fitting error of this fit. The blue line is a second degree polynomial fit to the local slopes. The green point is the extrapolated slope at the tropopause.

ACPD
13, 4221–4287, 2013

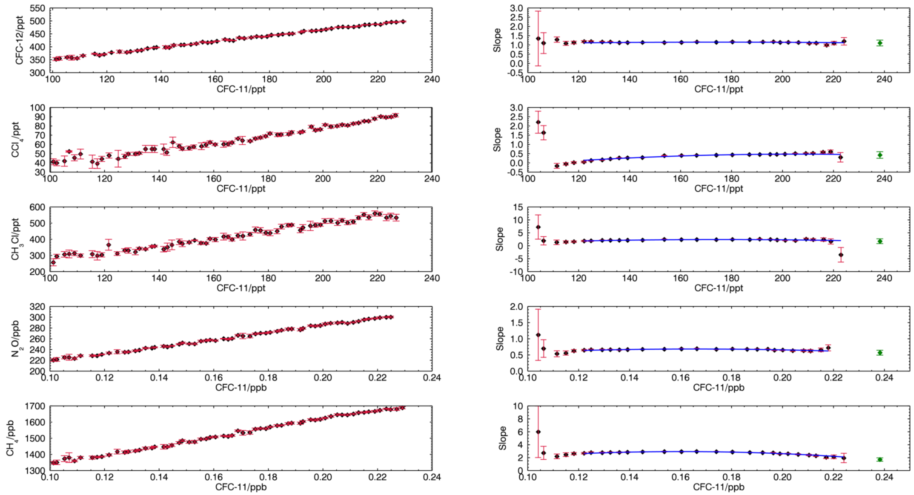

Fig. B12. Correlations between the volume mixing ratios of CFC-12, CCl_4, CH_4, CH_3Cl and N_2O and CFC-11 for the data from the Southern Hemisphere during the stratospheric summer of 2007. Left panels: the mean correlation profile. Each point represents the mean of the VMR in a window of 2 ppt of CFC-11. The error on these points is the standard deviation of the data within each 2 ppt window. Right panels: the local slope of data in an 80 ppt of CFC-11 window. The error on the points is the fitting error of this fit. The blue line is a second degree polynomial fit to the local slopes. The green point is the extrapolated slope at the tropopause.

ACPD
13, 4221–4287, 2013

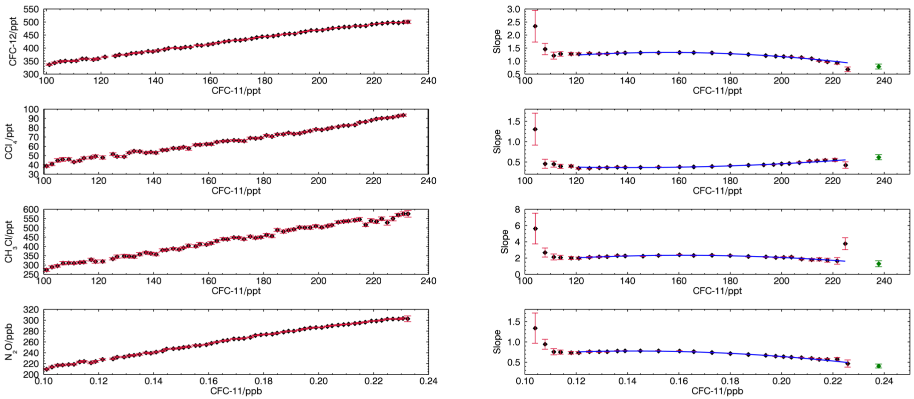

Fig. B13. Correlations between the volume mixing ratios of CFC-12, CCl_4, CH_3Cl and N_2O and CFC-11 for the data from the Southern Hemisphere during the stratospheric summer of 2008. Left panels: the mean correlation profile. Each point represents the mean of the VMR in a window of 2 ppt of CFC-11. The error on these points is the standard deviation of the data within each 2 ppt window. Right panels: the local slope of data in an 80 ppt of CFC-11 window. The error on the points is the fitting error of this fit. The blue line is a second degree polynomial fit to the local slopes. The green point is the extrapolated slope at the tropopause.

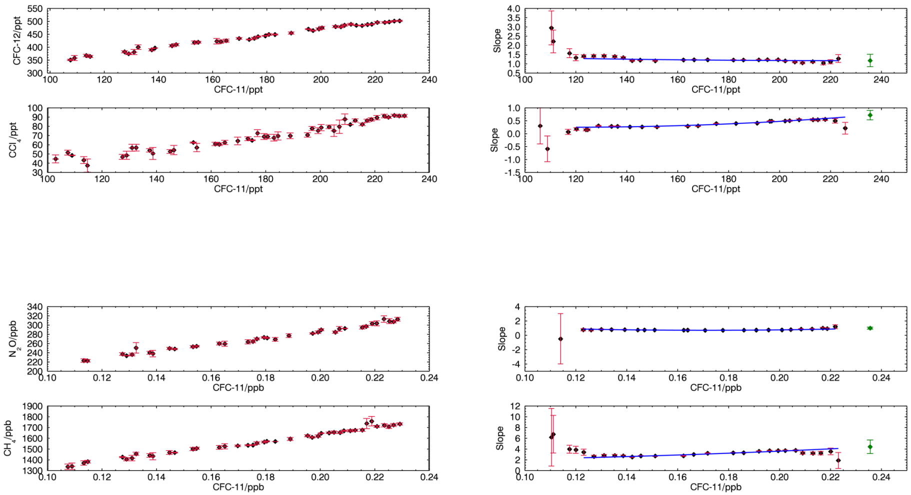

Fig. B14. Correlations between the volume mixing ratios of CFC-12, CCl_4, CH_4 and N_2O and CFC-11 for the data from the Southern Hemisphere during the stratospheric summer of 2009. Left panels: the mean correlation profile. Each point represents the mean of the VMR in a window of 2 ppt of CFC-11. The error on these points is the standard deviation of the data within each 2 ppt window. Right panels: the local slope of data in an 80 ppt of CFC-11 window. The error on the points is the fitting error of this fit. The blue line is a second degree polynomial fit to the local slopes. The green point is the extrapolated slope at the tropopause.

ACPD
13, 4221–4287, 2013

ACPD
13, 4221–4287, 2013

Stratospheric lifetimes of CFC-12, CCl_4, CH_4, CH_3Cl and N_2O

A. T. Brown et al.

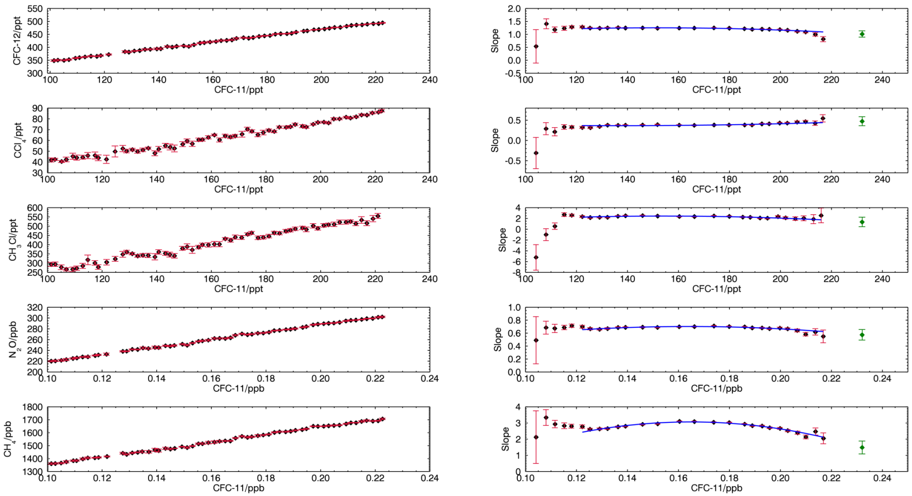

Fig. B15. Correlations between the volume mixing ratios of CFC-12, CCl_4, CH_4, CH_3Cl and N_2O and CFC-11 for the data from the Southern Hemisphere during the stratospheric summer of 2010. Left panels: the mean correlation profile. Each point represents the mean of the VMR in a window of 2 ppt of CFC-11. The error on these points is the standard deviation of the data within each 2 ppt window. Right panels: the local slope of data in an 80 ppt of CFC-11 window. The error on the points is the fitting error of this fit. The blue line is a second degree polynomial fit to the local slopes. The green point is the extrapolated slope at the tropopause.

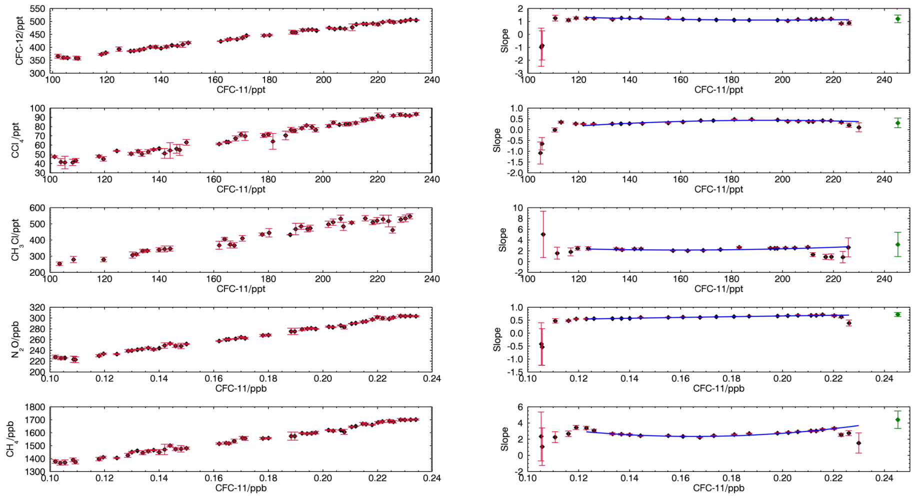

Fig. B16. Correlations between the volume mixing ratios of CFC-12, CCl_4, CH_4, CH_3Cl and N_2O and CFC-11 for the data from the Southern Hemisphere during the stratospheric winter of 2005. Left panels: the mean correlation profile. Each point represents the mean of the VMR in a window of 2 ppt of CFC-11. The error on these points is the standard deviation of the data within each 2 ppt window. Right panels: the local slope of data in an 80 ppt of CFC-11 window. The error on the points is the fitting error of this fit. The blue line is a second degree polynomial fit to the local slopes. The green point is the extrapolated slope at the tropopause.

ACPD
13, 4221–4287, 2013

Stratospheric lifetimes of CFC-12, CCl_4, CH_4, CH_3Cl and N_2O

A. T. Brown et al.

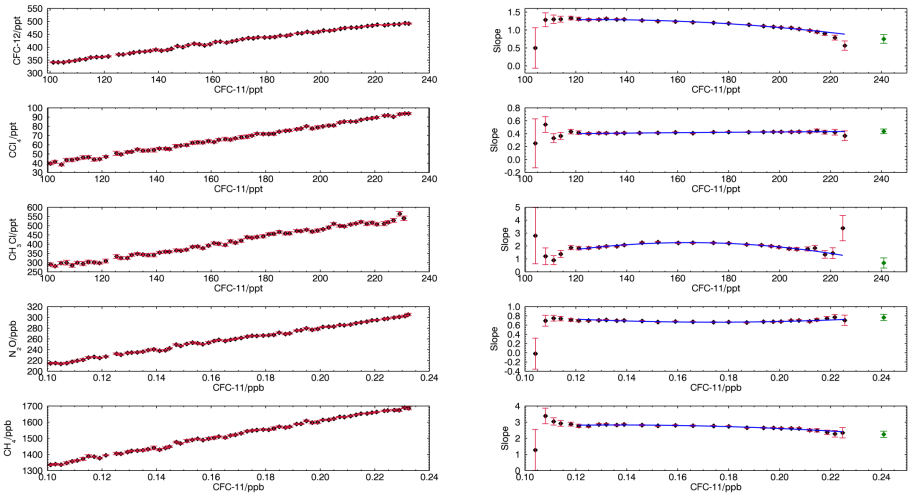

Fig. B17. Correlations between the volume mixing ratios of CFC-12, CCl_4, CH_4, CH_3Cl and N_2O and CFC-11 for the data from the Southern Hemisphere during the stratospheric winter of 2006. Left panels: the mean correlation profile. Each point represents the mean of the VMR in a window of 2 ppt of CFC-11. The error on these points is the standard deviation of the data within each 2 ppt window. Right panels: the local slope of data in an 80 ppt of CFC-11 window. The error on the points is the fitting error of this fit. The blue line is a second degree polynomial fit to the local slopes. The green point is the extrapolated slope at the tropopause.

ACPD
13, 4221–4287, 2013

Stratospheric lifetimes of CFC-12, CCl_4, CH_4, CH_3Cl and N_2O

A. T. Brown et al.

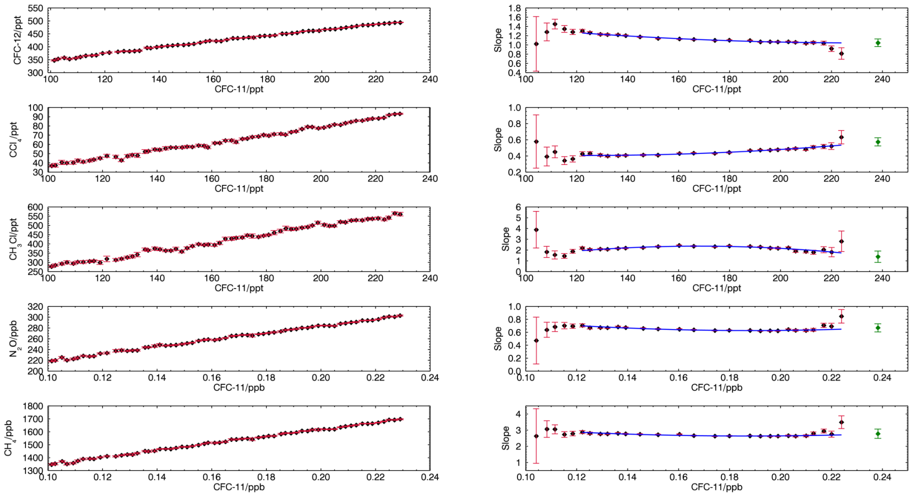

Fig. B18. Correlations between the volume mixing ratios of CFC-12, CCl_4, CH_4, CH_3Cl and N_2O and CFC-11 for the data from the southern hemisphere during the stratospheric winter of 2007. Left panels: the mean correlation profile. Each point represents the mean of the VMR in a window of 2 ppt of CFC-11. The error on these points is the standard deviation of the data within each 2 ppt window. Right panels: the local slope of data in an 80 ppt of CFC-11 window. The error on the points is the fitting error of this fit. The blue line is a second degree polynomial fit to the local slopes. The green point is the extrapolated slope at the tropopause.

ACPD
13, 4221–4287, 2013

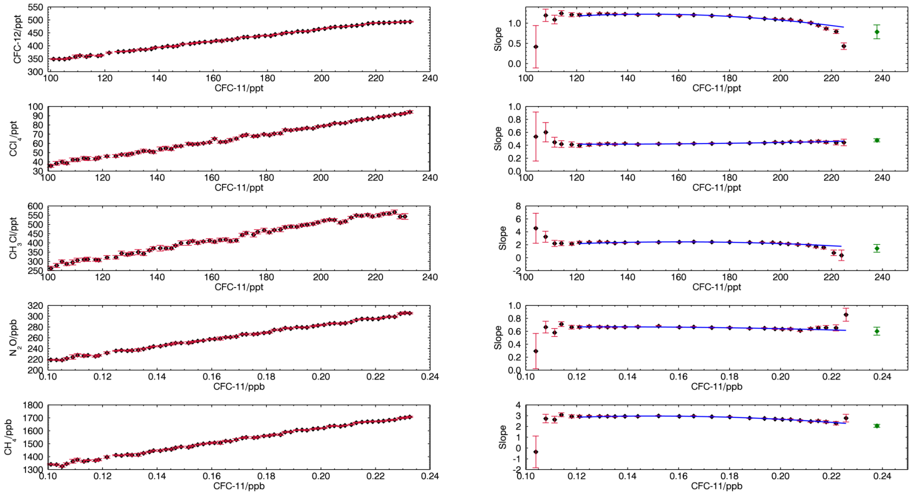

Fig. B19. Correlations between the volume mixing ratios of CFC-12, CCl_4, CH_4, CH_3Cl and N_2O and CFC-11 for the data from the southern hemisphere during the stratospheric winter of 2008. Left panels: the mean correlation profile. Each point represents the mean of the VMR in a window of 2 ppt of CFC-11. The error on these points is the standard deviation of the data within each 2 ppt window. Right panels: the local slope of data in an 80 ppt of CFC-11 window. The error on the points is the fitting error of this fit. The blue line is a second degree polynomial fit to the local slopes. The green point is the extrapolated slope at the tropopause.

ACPD
13, 4221–4287, 2013

Stratospheric lifetimes of CFC-12, CCl_4, CH_4, CH_3Cl and N_2O

A. T. Brown et al.

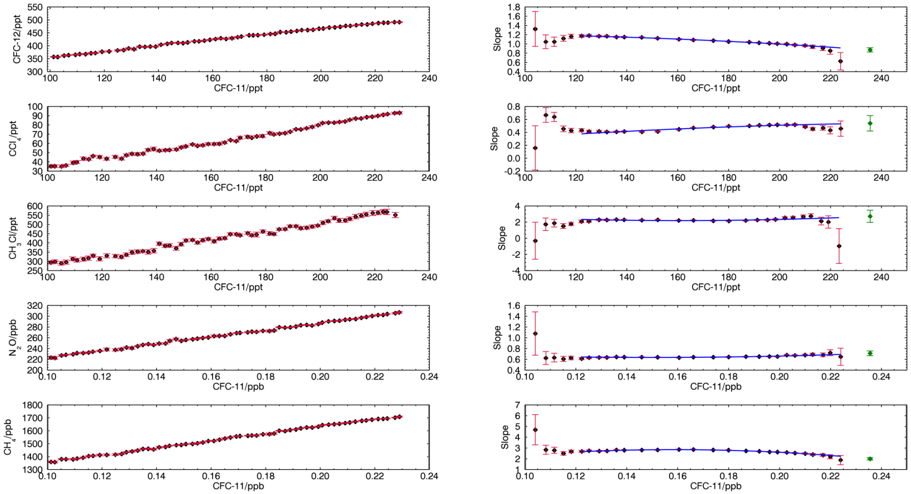

Fig. B20. Correlations between the volume mixing ratios of CFC-12, CCl_4, CH_4, CH_3Cl and N_2O and CFC-11 for the data from the southern hemisphere during the stratospheric winter of 2009. Left panels: the mean correlation profile. Each point represents the mean of the VMR in a window of 2 ppt of CFC-11. The error on these points is the standard deviation of the data within each 2 ppt window. Right panels: the local slope of data in an 80 ppt of CFC-11 window. The error on the points is the fitting error of this fit. The blue line is a second degree polynomial fit to the local slopes. The green point is the extrapolated slope at the tropopause.

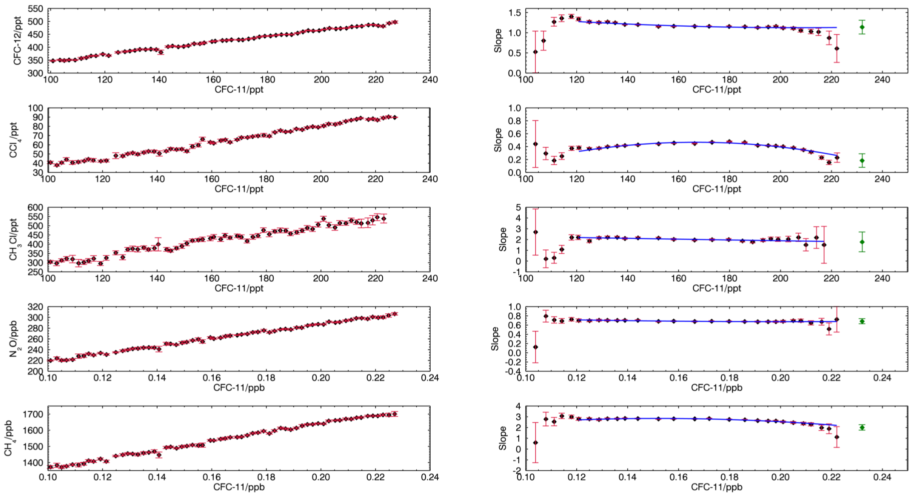

Fig. B21. Correlations between the volume mixing ratios of CFC-12, CCl_4, CH_4, CH_3Cl and N_2O and CFC-11 for the data from the southern hemisphere during the stratospheric winter of 2010. Left panels: the mean correlation profile. Each point represents the mean of the VMR in a window of 2 ppt of CFC-11. The error on these points is the standard deviation of the data within each 2 ppt window. Right panels: the local slope of data in an 80 ppt of CFC-11 window. The error on the points is the fitting error of this fit. The blue line is a second degree polynomial fit to the local slopes. The green point is the extrapolated slope at the tropopause.

ACPD
13, 4221–4287, 2013

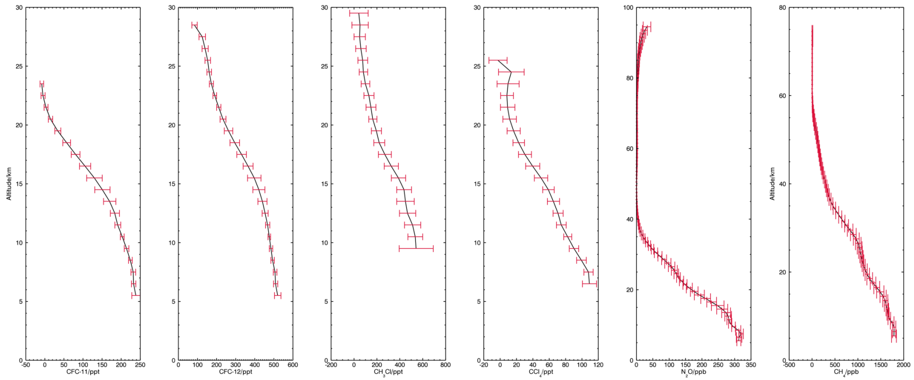

Fig. C1. The mean vertical profile of CFC-11, CFC-12, CH_3Cl, CH_4 and N_2O, calculated using data from 2009 between 90° and 75° N.

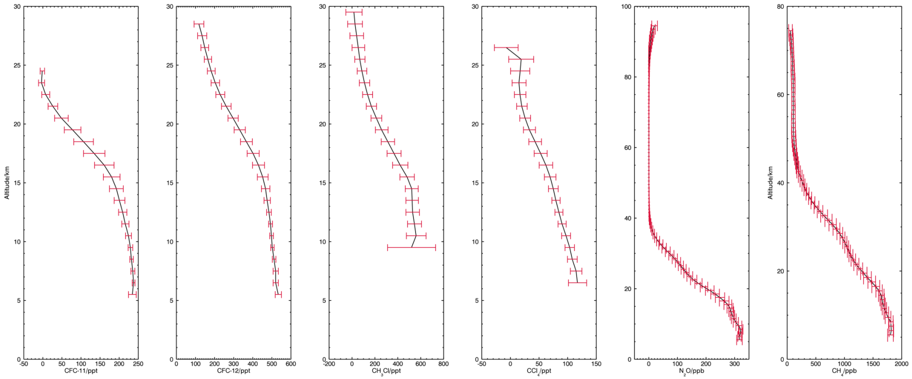

Fig. C2. The mean vertical profile of CFC-11, CFC-12, CH_3Cl, CH_4 and N_2O, calculated using data from 2009 between 75° and 60° N.

ACPD
13, 4221–4287, 2013

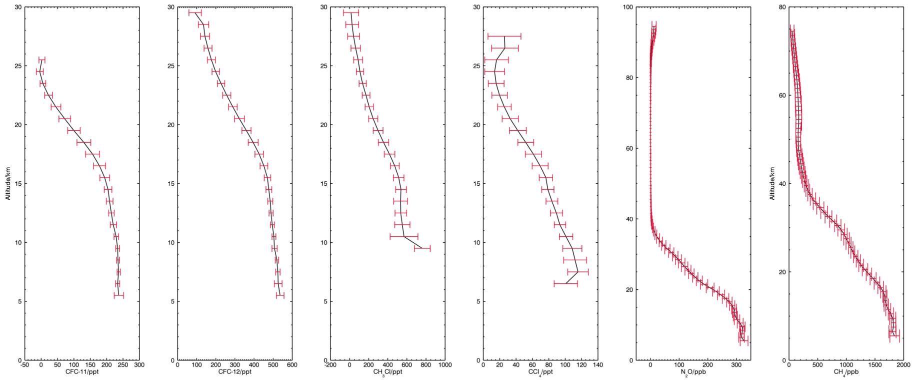

Fig. C3. The mean vertical profile of CFC-11, CFC-12, CH_3Cl, CH_4 and N_2O, calculated using data from 2009 between 60° and 45° N.

ACPD
13, 4221–4287, 2013

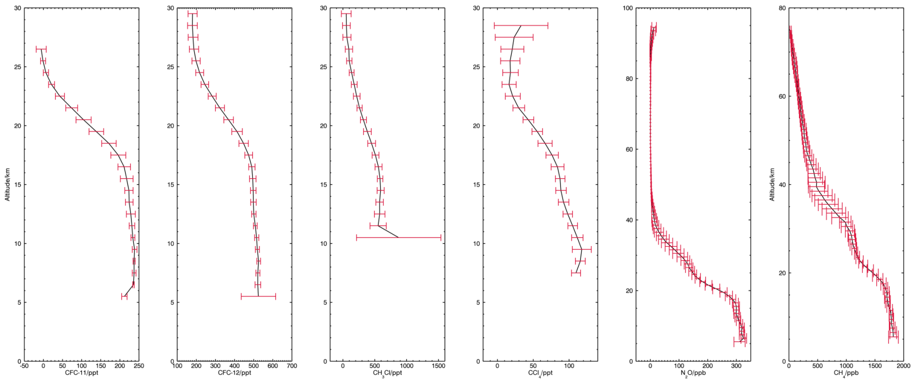

Fig. C4. The mean vertical profile of CFC-11, CFC-12, CH_3Cl, CH_4 and N_2O, calculated using data from 2009 between 45° and 30° N.

ACPD
13, 4221–4287, 2013

Stratospheric lifetimes of CFC-12, CCl_4, CH_4, CH_3Cl and N_2O

A. T. Brown et al.

Title Page
Abstract | Introduction
Conclusions | References
Tables | Figures
◀| |▶
◀ ▶
Back | Close
Full Screen / Esc
Printer-friendly Version
Interactive Discussion

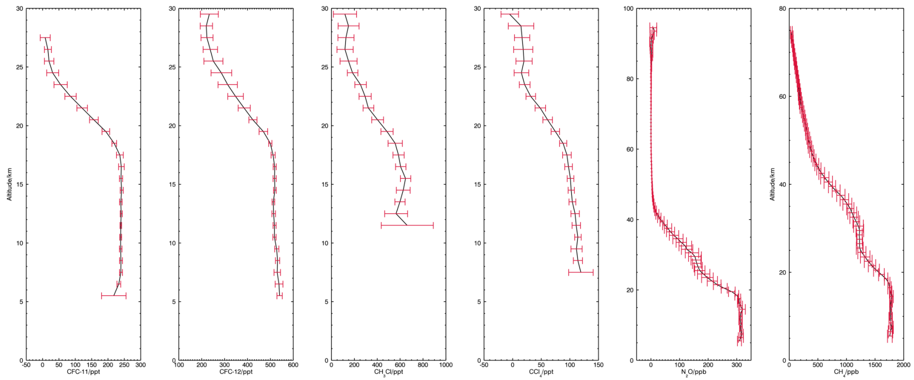

Fig. C5. The mean vertical profile of CFC-11, CFC-12, CH_3Cl, CH_4 and N_2O, calculated using data from 2009 between 30° and 15° N.

ACPD
13, 4221–4287, 2013

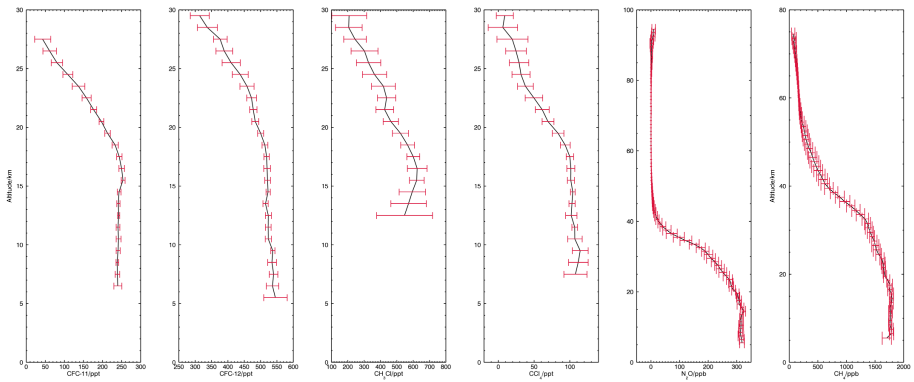

Fig. C6. The mean vertical profile of CFC-11, CFC-12, CH_3Cl, CH_4 and N_2O, calculated using data from 2009 between 15° and 0° N.

ACPD
13, 4221–4287, 2013

Stratospheric lifetimes of CFC-12, CCl_4, CH_4, CH_3Cl and N_2O

A. T. Brown et al.

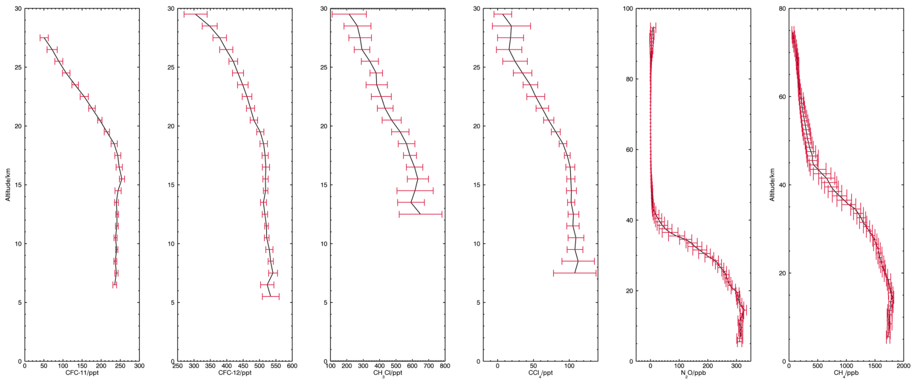

Fig. C7. The mean vertical profile of CFC-11, CFC-12, CH_3Cl, CH_4 and N_2O, calculated using data from 2009 between 0° and 15° S.

ACPD
13, 4221–4287, 2013

Stratospheric lifetimes of CFC-12, CCl_4, CH_4, CH_3Cl and N_2O

A. T. Brown et al.

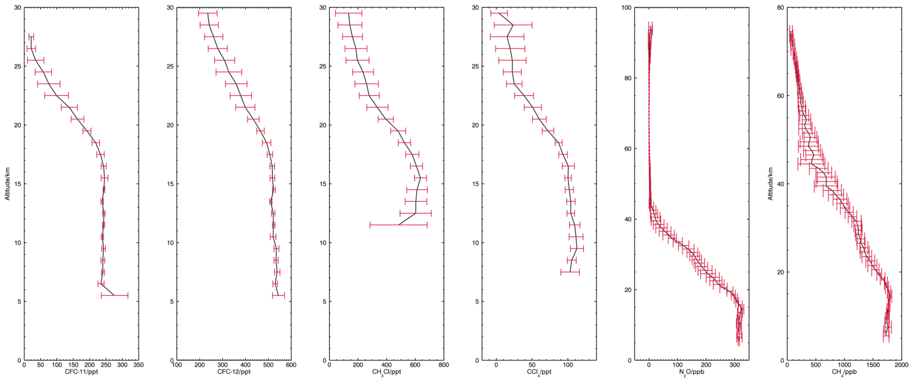

Fig. C8. The mean vertical profile of CFC-11, CFC-12, CH_3Cl, CH_4 and N_2O, calculated using data from 2009 between 15° and 30° S.

ACPD
13, 4221–4287, 2013

Stratospheric lifetimes of CFC-12, CCl_4, CH_4, CH_3Cl and N_2O

A. T. Brown et al.

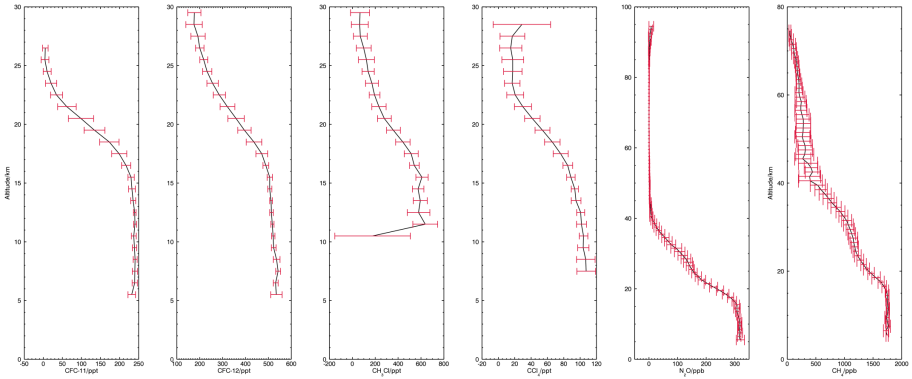

Fig. C9. The mean vertical profile of CFC-11, CFC-12, CH_3Cl, CH_4 and N_2O, calculated using data from 2009 between 30° and 45° S.

ACPD
13, 4221–4287, 2013

Title Page
Abstract | Introduction
Conclusions | References
Tables | Figures
◀| |▶
◀ ▶
Back | Close
Full Screen / Esc
Printer-friendly Version
Interactive Discussion

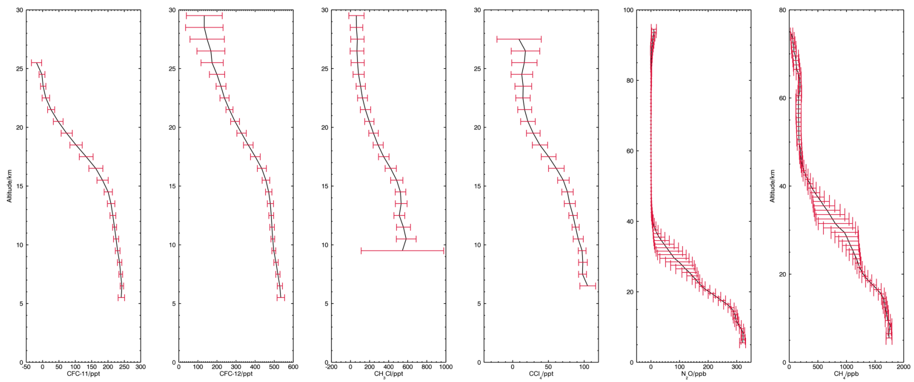

Fig. C10. The mean vertical profile of CFC-11, CFC-12, CH_3Cl, CH_4 and N_2O, calculated using data from 2009 between 45° and 60° S.

ACPD
13, 4221–4287, 2013

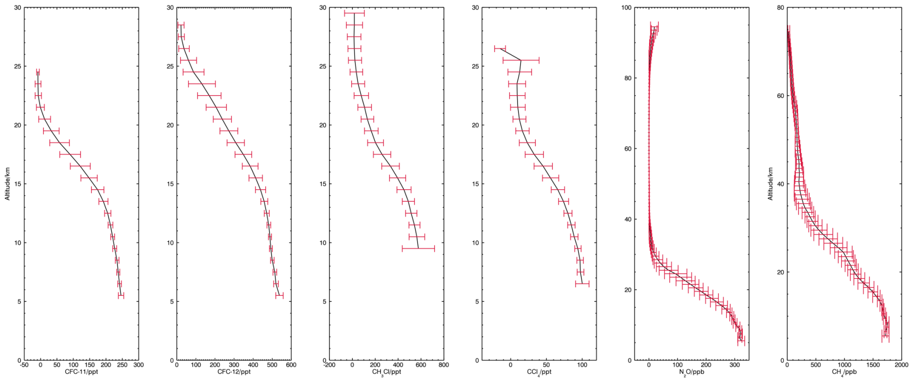

Fig. C11. The mean vertical profile of CFC-11, CFC-12, CH_3Cl, CH_4 and N_2O, calculated using data from 2009 between 60° and 75° S.

ACPD
13, 4221–4287, 2013

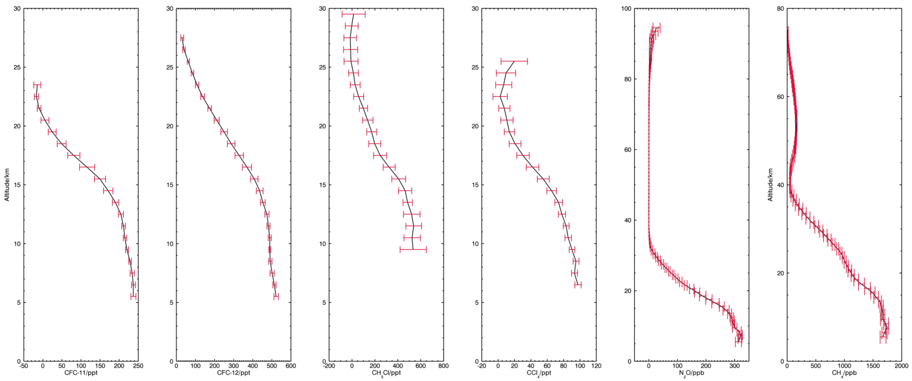

Fig. C12. The mean vertical profile of CFC-11, CFC-12, CH_3Cl, CH_4 and N_2O, calculated using data from 2009 between 75° and 90° S.

ACPD

13, 4221–4287, 2013

Stratospheric lifetimes of CFC-12, CCl_4, CH_4, CH_3Cl and N_2O

A. T. Brown et al.